CHALMERS
UNIVERSITY OF TECHNOLOGY

Interactions between DNA and the Parkinson's disease protein, α-synuclein

An investigation of secondary structure and aggregation of α-synuclein, induced by DNA

Master's thesis in Materials Chemistry

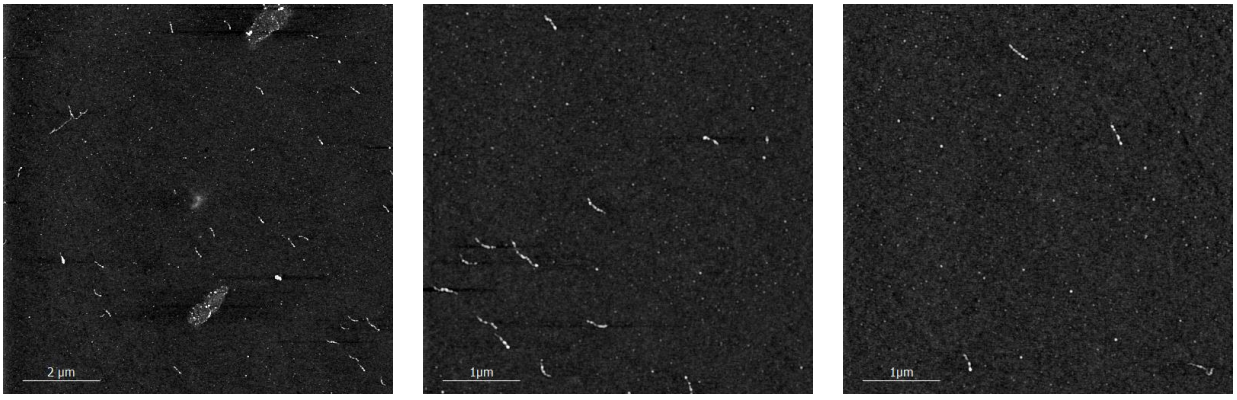

ALVINA WESTLING

Department of Biology and Biological Engineering
CHALMERS UNIVERSITY OF TECHNOLOGY
Gothenburg, Sweden 2018

Master's thesis 2018

Interactions between DNA and the Parkinson's disease protein, α-synuclein

An investigation of secondary structure and aggregation of α-synuclein, induced by DNA

ALVINA WESTLING

CHALMERS
UNIVERSITY OF TECHNOLOGY

Department of Biology and Biological Engineering
Division of Chemical Biology
Pernilla Wittung Stafshede's group
Chalmers University of Technology
Gothenburg, Sweden 2018

Interactions between DNA and the Parkinson's disease protein, α-synuclein
An investigation of secondary structure and aggregation of α-synuclein, induced by DNA
ALVINA WESTLING

Supervisor: Sandra Rocha, Researcher; Biology and Biological Engineering, Chemical Biology.
Examiner: Pernilla Wittung Stafshede, Head of the Chemical Biology Division in the Biology and Biological Engineering Department.

Master's Thesis 2018
Department of Biology and Biological Engineering
Division of Chemical Biology
Pernilla Wittung Stafshede's group
Chalmers University of Technology
SE-412 96 Gothenburg
Telephone +46 31 772 1000

Cover: Image of DNA molecules coated with α-synuclein on a surface of silica, taken with an atomic force microscopy by Kai Jiang.

Typeset in LaTeX
Gothenburg, Sweden 2018

Interactions between DNA and the Parkinson's disease protein, α-synuclein
An investigation of secondary structure and aggregation of α-synuclein, induced by DNA
ALVINA WESTLING
Department of Biology and Biological Engineering
Chalmers University of Technology

Abstract

With an increasing life expectancy, a deeper knowledge of neurodegenerative age-related diseases, such as Parkinson's disease (PD), has become of great importance. The main pathological feature of PD is the degeneration of neuromelanin-containing neurons (NCN) in the part of the brain controlling the involuntary movement of skeletal muscles. The degeneration of the NCN are shown to be linked to toxic aggregation species of α-synuclein (αS), which is a protein found in the brain and is believed to regulate the synaptic activity in the brain. αS has also been observed in the cytoplasm and nucleus and there are suggestions that structural changes can be induced in αS by binding with DNA, but there are only a few studies on αS-DNA interactions. This thesis therefore aims to obtain a deeper understanding of the role of protein-DNA interactions in vitro, to enable for the possibility that αS-DNA interactions may have some participation in PD. For example, in relation to the gene regulation. To investigate the interactions, synthesised wild-type αS has been studied in bulk phase as well as at a single molecule level, with four types of commercially available DNA sequences. In studies in the bulk phase, with linear dichroism, interactions between protein and DNA were observed. Secondary structural changes in αS and DNA was not evident in linear dichroism and circular dichroism experiments. To investigate the protein-DNA interactions at a single molecule level, nanofluidic channels and atomic force microscopy were used. It was then observed that the interactions between αS and DNA induce a stiffer configuration in the DNA molecules, causing an elongation in length of 30%. The increase in length of the DNA molecules after interactions with αS could be of interest when further investigating the gene-regulating role of αS. Images of the interactions also revealed that the binding of αS to DNA appears in small clusters along the DNA molecule, suggesting that there are favourable αS binding sites on the DNA molecule.

Keywords: Parkinson's disease, α-synuclein, α-synuclein aggregates, DNA, protein-DNA interactions.

Acknowledgements

When one asks for advice for the future regarding employment and workplace, most people answer that the supervisor and the boss are the most important parts of the new job. If one feels comfortable with them, it will turn in to a good workplace. After five months working on this thesis at Chemical Biology I fully agree, the knowledge, support and kindness I have received from my supervisor Sandra and from Pernilla, together with her group, have been invaluable. Special thanks to you and the whole group for this opportunity. There also has to be a special thanks to Kai Jiang for supervising me and for sharing his knowledge of the instruments I have used in single molecule studies, together with helping me obtain a majority of the data presented in this thesis.

It is not often I get the opportunity to write acknowledgement and I will, therefore, without hesitation, take this chance to thank my friends and family for their tireless support. And thanks to those of you who, in addition to that, have helped me by reading this thesis and removing all signs of my poor feeling of sentence structure.

Alvina Westling, Gothenburg, June 2018

Contents

List of abbreviations and symbols

A	Adenine
A	Absorbance
AFM	Atomic Force Microscopy
αS	α-synuclein
bp	Base Pairs
BME	β-Mercaptoetanol
C	Cytosine
c	Speed of light (299 792 458 m/s)
c	Molar concentration [M]
CD	Circular Dichroism
ctDNA	Calf Thymus DNA
DNA	Deoxyribonucleic Acid
E	Electric field [N/C]
E	Energy [J]
E_L	Electric field in left direction [N/C]
E_R	Electric field in right direction [N/C]
G	Guanine
GFC	Gel Filtration Chromatography
h	Planck's constant (6.63×10^{-34} Js)
I	Intensity after the sample [W/m^2]
I_0	Intensity before the sample [W/m^2]
l	Length of cuvette [cm]
λ	Wavelength [nm]
LB	Lewy Body
LN	Lewy Neurites
N	Number of peptide bonds
NC	Nanofluidic Channels
NCN	Neuromelanin-Containing Neurons
PD	Parkinson's Disease
ϕ	Angle around the N-Cα bond
ψ	Angle around the Cα-C bond
T	Thymine
TE-buffer	Tris-EDTA buffer solution
ThT	Thioflavin T
θ_{MRE}	Ellipticity based on the molar concentration [deg/(m*M)]
θ_{obs}	Observed CD signal [degrees]
v	Frequency [s^{-1}]
YOYO	YOYO-1

List of Figures

List of Tables

1
Introduction

Parkinson's disease (PD) is a common neurodegenerative age-related disease that causes impairment in both physical and mental health. A protein that has been closely linked to PD, but of which there is still limited understanding of its role in the onset of the disease, is α-synuclein (αS). This chapter gives some general background about PD and αS in order to introduce the main focus of this thesis; the study of the interactions between αS and DNA. The overall aim and limitations of the thesis are also presented in this chapter.

1.1 Background

PD is together with Alzheimer's disease one of the most common neurodegenerative diseases in the world. PD is an age-related disease estimated to affect 1% of all people at the age of 70 but it is also seen in the younger population [1]. The cause of the disease is still unknown to an extent, but it is believed to be caused by both genetic and environmental factors. The symptoms of PD are generally developing slowly, the most common of which are tremors, akinesia, bradykinesia, stiffness and depression [1, 2]. The symptoms become more severe with time but owing to medications that ease the symptoms, people with PD can usually lead a normal life for several years. There is today no known cure to PD.

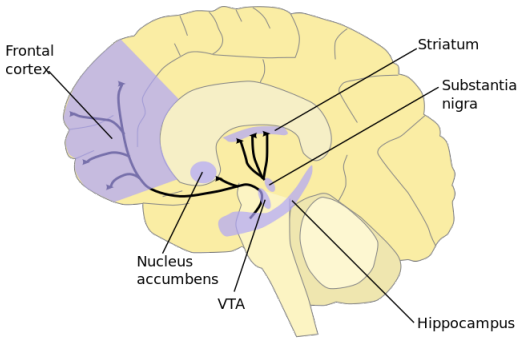

Figure 1.1: Illustration of the human brain showing the location of the substantia nigra which plays an important role in the movement of skeletal muscles and which is severely affected in PD [3]. Image available under the public domain.

The main pathological feature of PD is the degeneration of neuromelanin-containing neurons (NCN) in the part of the brain called substantia nigra, see Figure 1.1, which controls the involuntary movement of skeletal muscles. The neurons in the substantia nigra synthesise dopamine and a reduction of these will create a dopamine deficiency which gives rise to the symptoms of PD [1, 2, 4]. The drugs used to treat the symptoms of PD increase the concentration of dopamine either by stimulating the dopamine receptors or by adding more of it [5].

Examination of the substantia nigra in a PD patient will not only show a marked decrease in the number of NCN, but also the presence of Lewy bodies and Lewy neurites. Lewy bodies (LB) are abnormal aggregates of proteins inside the nerve cells and Lewy neurites (LN) are abnormal neurites of aggregated protein, similar to those found in LB. The major component in LB and LN is αS and these aggregates of protein are the pathological hallmark of idiopathic PD [1, 2, 4]. The association between Lewy pathology and the pathogenesis of the disease is not yet fully understood.

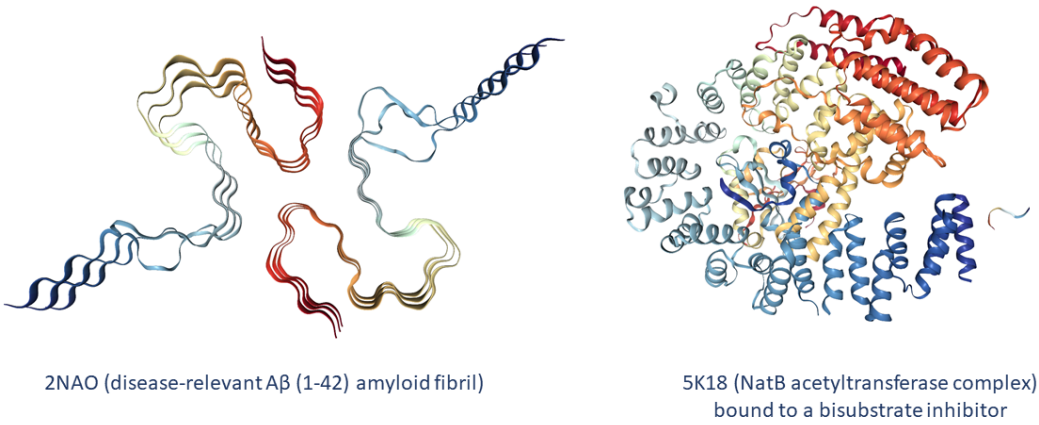

Figure 1.2: Example of the secondary structures of β-sheets and α-helix (β-sheets in 2NAO and α-helix in 5K18). Image created in *PV* a WebGL based 3D program at *RCSB Protein Data Bank*.

αS was discovered in 1988, and was related to neurodegenerative diseases, such as PD, at an early stage [6, 7]. The normal physiological functions of αS are still unknown, but today they are believed to play an important part in the regulation of synaptic activity and possibly also in gene regulation [8, 9]. When symptoms of PD are experienced, the aggregated form of αS, in the form of LB and NB, can be found in the brain. In the native form, αS is an unordered protein but when aggregated or bound to micells, a more ordered structure is obtained. When αS gets associated with lipid vesicles it obtains an α-helical structure and amyloid formation involves β-sheet structure formation of αS [10]. Figure 1.2 illustrates examples of β-sheet structure and α-helix structure. Studies on PD suggest several underlying causes of the disease-causing folding of αS, for example, the presence of metal ions creating oxidative stress or the presence of some pesticides [11, 12]. Recently some research has indicated that interactions between αS and DNA could give rise to structural

changes as well [13].

1.2 Aim and objectives of this thesis

The aim of the thesis is to obtain a deeper understanding of protein-DNA interactions in studies performed *in vitro*. This to enable for the possibility that αS may have some additional participation in PD, for example by association with gene regulation. The project aims to study the interaction between αS and DNA and to identify how the expected binding of αS to DNA promotes structural changes in both DNA and αS. To more easily create a clear vision of the thesis and design the experimental work, the aim of the thesis has been specified into the following questions:

- Can interactions between αS and DNA be seen *in vitro* in bulk phase?
- Can interactions between αS and DNA be seen *in vitro* at a single molecule level?
- What structural changes can be seen in αS and in DNA when interacting with each other?
- Does αS have higher affinity to specific DNA sequences?

1.3 Methodology

This thesis is based on laboratory work focused on the interaction between DNA and αS. Previous research on the topic is reviewed in Chapter 2. To obtain information about the interactions and structural changes in αS and DNA, four main methods have been used; absorbance spectroscopy, fluorescence spectroscopy, nanochannel microfluidics and atomic force microscopy. The theoretical backgrounds to these methods are presented in Chapter 2 and the specific laboratory method is found in Chapter 3. The results and discussion regarding the results from the laboratory work are presented in Chapter 4 together with Appendix.

The topic of this thesis is part of a project carried out in a research group involving the researchers Pernilla Wittung Stafshede, Fredrik Westerlund, Kai Jiang and Sandra Rocha. The work has resulted in a paper that is under preparation and will include parts of the data obtained during the thesis.

1.4 Delimitations

To investigate the interactions between αS and DNA, wild-type αS has been studied together with four types of DNA sequences of different base pair (bp) length. All samples of wild-type αS used in the thesis were synthesised at Chalmers by Ranjeet

Kumar. The four types of double-stranded DNA used were: λ-DNA (48 kbp long), calf thymus DNA (ctDNA, 8-15 kbp long), 1k DNA (1 kbp long) and 10k DNA (10 kbp long). λ-DNA is suitable for studies using nanofluidic channels but too long to use in linear dichroism and atomic force microscopy techniques; ctDNA was therefore used in experiments with linear dichroism, circular dichroism and aggregation experiments. 10k DNA and 1k DNA are studied as single molecules with nanofluidic channels and atomic force microscopy. The main limitation of this project is the decision of only investigate wild-type αS and no mutations. If mutations of αS were to be studied more information about the behaviour of αS could be obtained, such as which protein binding sites are involved.

2

Theory

Chapter 2 presents fundamental information about the link between PD, αS and DNA. Here previous research on the topic is reviewed, together with information about the laboratory methods used.

2.1 Theoretical background of proteins and DNA

This section of the thesis explains some general background of proteins and DNA, with focus on their structures.

2.1.1 Proteins and their structures

Proteins are large biomolecules taking part in many important functions in the human body. Some functions of proteins are: DNA replication, transporting molecules and catalysing metabolic reactions. Proteins are made by condensation of amino acids which form peptide bonds [14]. There are several ways to categorise proteins regarding their structure, in Figure 2.1 are four of them schematically displayed. The order of amino acids in a sequence, of a protein, is called its primary structure. The folding pattern in a protein is called its secondary structure and it is determined by the torsion angles, which are the angles ϕ and ψ, see Figure 2.2. ϕ is the angle of the bond between the nitrogen atom and the α-carbon, ψ is the angle around the α-carbon and the β-carbon. The tertiary structure is determined by the folding of the protein chains in space. Association of folded polypeptide molecules to complex functional proteins results in a quaternary structure [15].

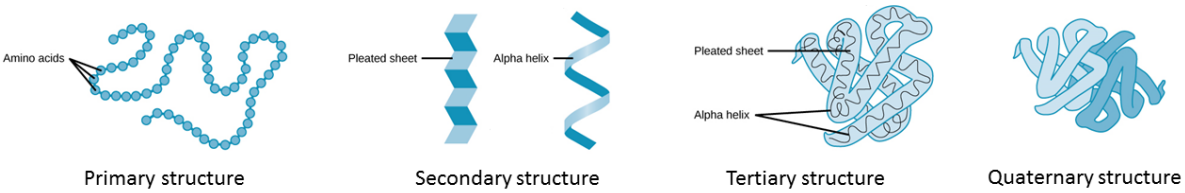

Figure 2.1: Illustration of four classification groups of protein structures; primary structure, secondary structure, tertiary structure and quaternary structure. Image available under CC-BY-4.0 [16].

Proteins differ from one another primarily in their sequence of amino acids, which is dictated by the nucleotide sequence of their genes, and which usually results in protein folding into a specific three-dimensional structure that determines its activity.

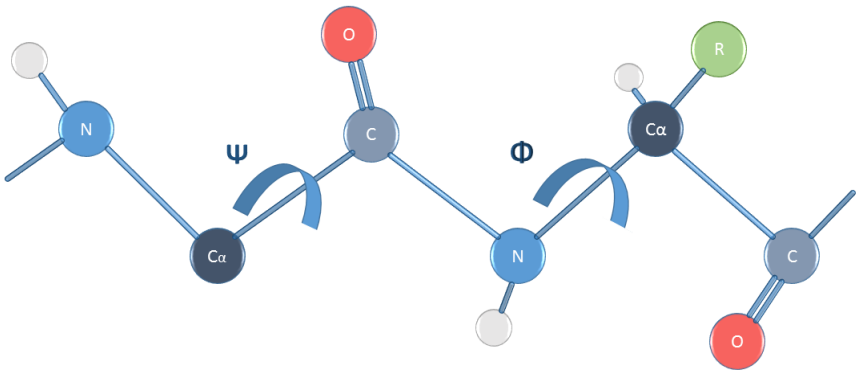

Figure 2.2: Schematic image of an unspecified polypeptide molecule displaying the angles ϕ and ψ, which determine the secondary structure of a protein.

There are several commonly occurring secondary structures of proteins: the α-helix, the β-sheet and the π-helix [15]. All these structures are determined by the angles ϕ and ψ. As an example, the α-helix structure has an angle of approximately 100° between successive residues with ϕ=-57° and ψ=-47°. It is hydrogen bonding within the molecule that makes the structure possible. When a protein is said to have an undefined structure is it called random coil. In the coils the amino acids still have a defined position even though it is often called a unordered structure [15, 17].

The structure of a protein is changeable by external forces. When the structure is changed so that the protein unfolds and loses its structure and consequently its function, it is a process known as denaturation. pH, temperature, salt concentration or solvent are some factors that affect the structure of proteins [15].

2.1.2 Structure of DNA

DNA molecules, where all genetic information of living cells is stored, are located inside cells, often only in the nucleus but sometimes also freely suspended in the cell. DNA molecules are built of nucleotides in a double-stranded chain-like structure, called the DNA-helix, see Figure 2.3. The nucleotide is composed of nitrogen-containing nucleobases, a phosphate group and sugar called deoxyribose. There are four types of nucleobases; guanine (G), cytosine (C), adenine (A) and thymine (T) [18, 19]. The nucleotides are joined together by covalent bonds between the nucleotides, the sugar and the phosphate group, which give rise to an alternating sugar-phosphate backbone. The nitrogenous bases of the two separate polynucleotide strands are bound together with hydrogen bonds, where C binds with G and A with T. The DNA molecule has an overall negative charge due to the phosphate groups [18].

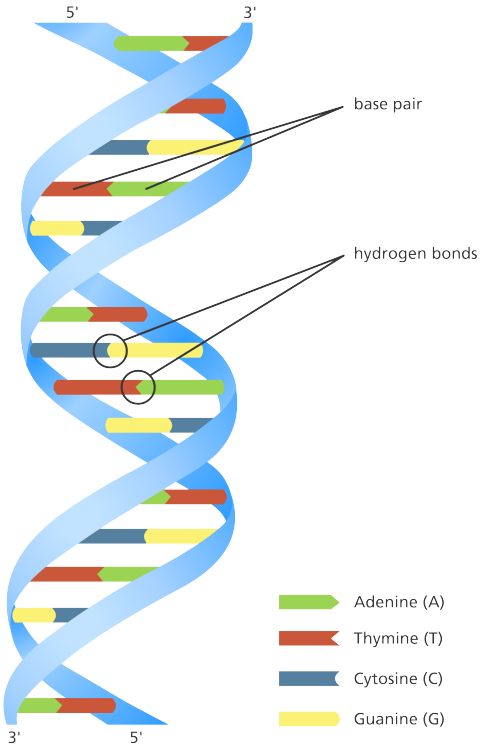

Figure 2.3: Schematic image of the secondary structure of the DNA-helix, viewing the four base pairs; guanine (G), cytosine (C), adenine (A) and thymine (T). Image created by Genome Research Limited, available under CC BY-NC-SA 2.0 [20].

The DNA-helix can exist in several possible conformations; A-DNA, B-DNA, and Z-DNA forms [19]. Of these, only B-DNA and Z-DNA have been directly observed in functional organisms, where B-DNA is the most common under the conditions found in cells. These three conformations differ in direction of the helical structure and in pattern. A-DNA and B-DNA have a right-handed double helical structure while Z-DNA has a left-handed helical structure. The A-DNA helix is wider than the B-DNA helix and with a difference in groove depth. The conformation that DNA adopts depends on the DNA sequence, hydration level, and surrounding environment among other factors.

2.2 Parkinson's disease and α-synuclein

PD is a neurodegenerative disease that affects the dopamine-producing neurons in the substantia nigra. The disease is characterised by large protein aggregates, referred to as LB [5]. The composition of LB is the aggregated form of the protein αS, which was linked to PD as early as 1988 [6, 21]. It was then concluded that LB occurs wherever there is an excessive loss of neurons. The research suggested that the cases of incidental LB disease are presymptomatic cases of PD, and confirmed the importance of age (time) in the evolution of the disease [21]. After this, there have been several other studies showing the importance and involvement of αS in

PD, and there are a number of strong pieces of evidence supporting this statement. For example, a mutation in the gene of αS was shown to be related to the familial case of early-onset PD and the production of wild-type αS in transgenic mice leads to motor complications and neuronal inclusions reminiscent of PD [4, 7, 22]. The normal physiological functions of αS are still unknown, but today they are believed to play an important part in the regulation of synaptic activity by controlling the neuronal levels of dopamine in the brain [8, 10]. The control of dopamine level is done by decreasing the activity of dopamine transporters. If this process works inefficiently there is a possibility that the increased levels of oxidative dopamine byproducts can damage the cells of the brain. A theory of the toxicity of αS aggregates is therefore that aggregates of αS cannot control the dopamine levels and thereby create neurotoxicity [10].

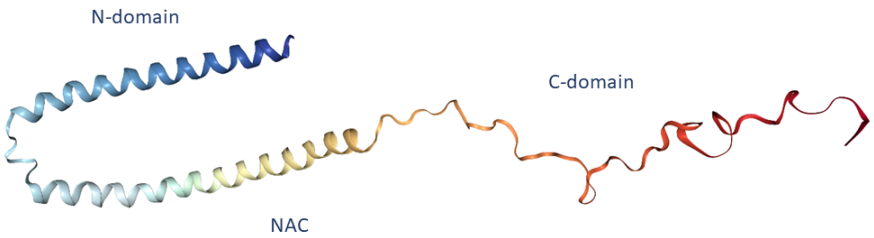

Figure 2.4: Secondary structure of αS when bound to micelles, created in *PV* a WebGL based 3D program at *RCSB Protein Data Bank* with indications of location of the three domains; N, NAC and C.

αS is a 140 amino acid long acidic protein, present in high concentrations at the presynaptic terminals and is found in both soluble and membrane-associated form in the brain [4, 6]. αS has three regions; the N-terminal domain which is the lipid binding α-helical part, the NAC which is the amyloid binding part and the C-terminal domain which is an acidic tail of the protein, see Figure 2.4 and Figure 2.5 [4, 10]. The N-terminal domain is positively charged and able to induce α-helical structure in the protein when bound to lipids. The NAC part of αS is shown to be involved in aggregation and formation of fibrils due to its ability to form cross β-structure [10]. It is believed that the random coil C-terminal domain takes part in the aggregation as well, by interactions with the NAC part. There are also suggestions that the C-terminal domain modifications might be involved in the pathology of αS. Around pH 7, αS has 24 negative charges, 15 of these are located in the C-terminal domain of the protein, making the protein less willing to fold itself at this pH, than if the surroundings were more acidic or alkaline. [23].

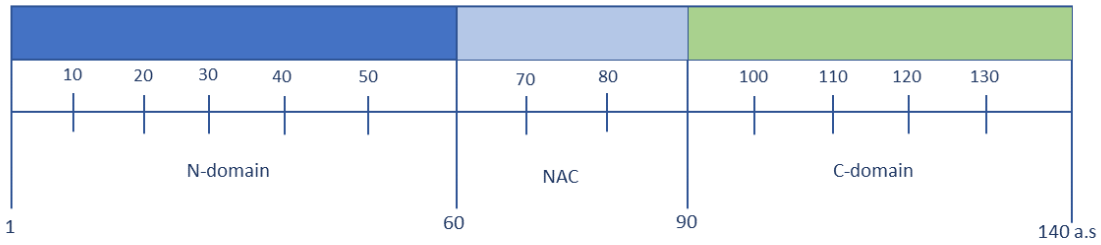

Figure 2.5: Schematic illustration of the domains of αS and their number of amino acids.

The aggregation and amyloid formation of proteins usually occur via intermediates [24]. In the case of αS there are several stages in the aggregation process, from monomer to LB, involving the formation of dimers and different types of oligomers. The aggregation process is strongly driven forward and reluctant to go back to a monomeric state, as illustrated by the arrows in Figure 2.6. In the aggregated state, αS has a β-sheet structure while the native structure is unordered with low overall hydrophobicity and large net charge [11].

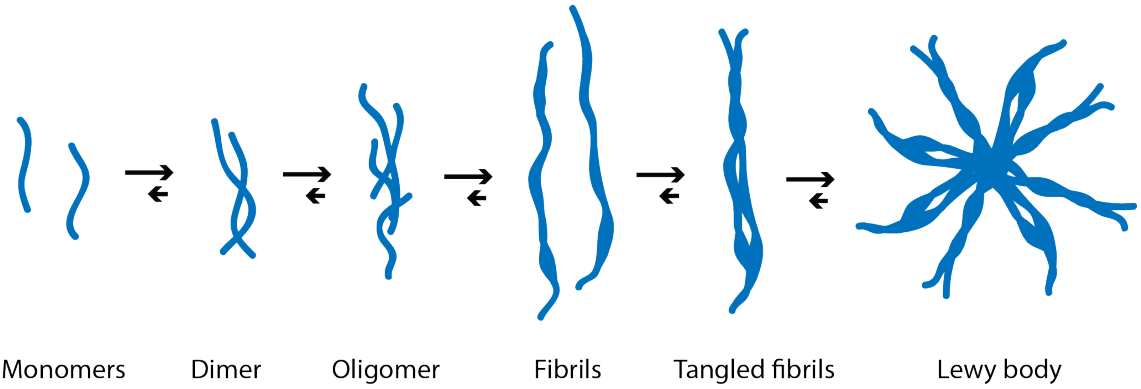

Figure 2.6: Illustration of aggregation of αS, showing the intermediates from monomers to Lewy body.

There are indications that the partially folded intermediate conformation is the most critical specie of aggregation process [11]. Oligomers of αS are present in the intermediate step and there is a possibility that these mostly contribute to the degradation of neurons and not the fully aggregated fibrils. Studies on a smaller and nonfibrillar αS aggregates showed that the nonfibrillar αS is neurotoxic and induces mitochondrial toxicity and fission as well as energetic stress, leading to cell death [25].

As mentioned previously is mostly the NAC part, which is the hydrophobic part of the protein, involved in the change of structure within αS [4, 26]. There is evidence that the unfolded structure of the protein corresponds to these characteristics of low hydrophobicity and charge, and that a change in the structure would disable

aggregation of the protein. The process of aggregation of αS is still being studied in detail by many in an attempt to identify the toxic species responsible for neurodegeneration. Studies on this topic suggest several underlying causes for the folding of αS, for example, binding to long chains of fatty acids, presence of some metal ions creating oxidative stress and also presence of some pesticides [11, 12]. Recently some research on DNA-protein interactions has indicated that interactions between αS and DNA could lead to structural changes in αS as well, and that αS also plays a gene-regulatory role in the cell nucleus. [9, 11, 13].

Overall, it is established that abnormal aggregates of αS occur early on in PD but there is no clear explanation for the initiation of the aggregation or which of the stages, if any, leads to the degeneration of neurons.

2.3 α-synuclein interacting with DNA

αS has been found in a aggregated state in the cell cytoplasm where it can take part in vesicle transport over membranes. In addition, αS has also been observed in the nucleus and it seems to be able to move between the cytoplasm and nucleus in a dynamic manner [27, 28]. A few studies show that αS interacts with DNA in the nucleus and that the binding occurs favourably to GC-box-like sequences via electrostatic interactions and may modify properties of both the protein and the DNA [8, 11, 12]. In the N-terminal domain of αS there are more positively charged lysine residues occurring than in the rest of the molecule, which suggests favourable DNA binding properties [24].

Using circular dichroism spectroscopy, it has been shown that αS binds strongly to supercoiled DNA [29]. This binding showed a change in conformation of the DNA, from β-form to altered β-form. It seems that αS induces DNA damage by changing its stability, its conformation and by causing DNA nicking. αS is also affected by these interactions, by undergoing a transition from unordered structure to α-helix and β-sheet structure [30]. When single-stranded DNA was mixed with αS an increase of 80% in α-helix content was observed [11]. In these experiments there have also been evidence that different types of DNA behave differently, most likely due to their GC content. Both λ-DNA and calf thymus DNA induce structural changes in αS, however, some differences can be seen which could be explained by the GC content. Calf thymus DNA has a GC content of approximately 70% and λ-DNA approximately 42% [24].

The amount of αS in the nucleus has been shown to be affected by oxidative stress. The fraction of αS increases upon chemically-stimulated oxidative stress and it was reported to modulate transcription of the master mitochondrial transcription activator called PGC1alpha [31]. The changes in transcription of PGC1alpha induced by αS negatively affected mitochondrial morphology and function. These studies clearly suggest that αS may have additional roles in PD that are related to nuclear gene regulation, which makes it an important and interesting topic for further research [8, 12].

2.4 Preparatory methods

The project aims to investigate how monomers of αS interact with DNA. As mentioned previously αS exists as monomers, dimers, oligomers and fibrils which makes the preparatory work of ensuring only monomers in the protein solution crucial.

2.4.1 Gel filtration chromatography

Gel filtration chromatography (GFC) is a method where proteins, peptides and DNA fractions are separated based on their molecular size [32, 33]. The separation is achieved by letting the molecules move with a mobile phase through a porous bed of gel, where they due to steric reasons diffuse unevenly into the bed. Smaller molecules diffuse further into the matrix and hence move slower through the column while larger molecules move more quickly through the column. Both molecular weight and three-dimensional shape contribute to the degree of retention [33].

At the exit zone of the column an in-line UV source is located, irradiating the eluate with light of specific wavelengths, suitable for detecting proteins [32]. Detecting the absorbance of the eluate provides information about the eluate which is gathered in fractions in tubes. The corresponding fractions of the separated compounds are identified by consulting the UV spectrum of absorbance. Figure 2.7 shows a characteristic graph from GFC, where the measuring wavelength was set to 280 nm and the peak indicates the presence of monomers in fraction 9 and 10.

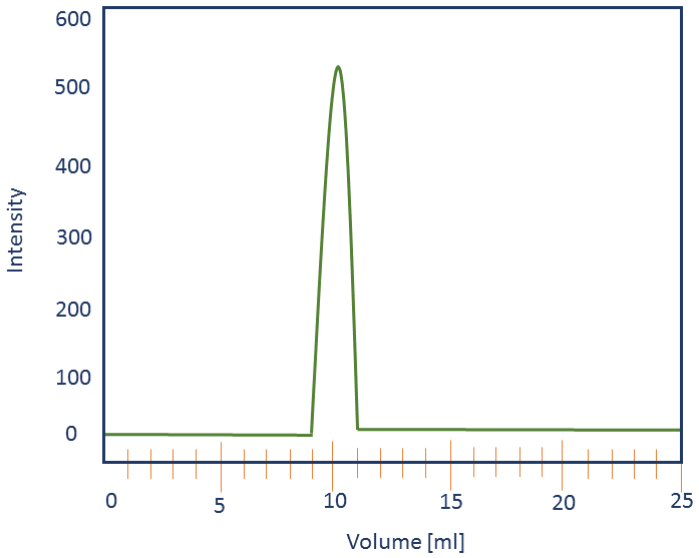

Figure 2.7: Characteristic graph from GFC purification of αS, showing in which fractions the protein is eluted.

2.5 Analysis methods

Several methods have been used to analyse and gain information about the samples in this project, both regarding DNA and protein configuration. The theories behind these methods are explained in this section.

2.5.1 Absorbance spectroscopy methods

A common way to obtain information about a sample is to apply the fact that molecules absorb light. In light absorbance spectroscopy methods, electromagnetic waves from the infrared, the visible and the ultraviolet region of the electromagnetic spectrum can be absorbed [34]. Absorbance spectroscopy is commonly used to detect a specific molecule or to determine the concentration of that molecule. In this project absorbance spectroscopy was used to determine the concentration. This is done by knowing at which characteristic wavelength the molecule absorbs light and then measure the absorbance. The absorbance can then be correlated to the concentration with Bouguer-Lambert-Beers law, see Equation 2.1 [35].

$$log(I_0/I) = A = \epsilon * l * c \tag{2.1}$$

Where I and I_0 are the intensity of the light beam before and after passing through the sample respectively. If divided and logarithmised they are known as the absorbance A. ϵ is the molar extinction coefficient or absorptivity of the molecule of interest [$M^{-1}cm^{-1}$], l is the length of the sample cuvette [cm] and c is the molar concentration [M] [36]. Proteins are known to absorb light at a wavelength of 280 nm due to the presence of tyrosine and tryptophan, and DNA at a wavelength of 260 nm [37]. For αS the molar extinction coefficient is estimated to be 5960 $M^{-1}cm^{-1}$ and for DNA 13200 M $bp^{-1}cm^{-1}$, which expresses the concentration in mol base pairs per volume [M bp].

Linear dichroism (LD) and circular dichroism (CD) are two spectroscopy methods commonly used when studying DNA and proteins. They are both based on the use of polarised light to obtain structural information about the molecules of interest. In polarised light, the electric field is no longer randomly distributed around the directional axis but collected in a single plane along the axis [38]. LD detects the difference in absorption between parallel polarised and perpendicular polarised light, and CD the difference in absorption between left and right polarised light, which is schematically illustrated in Figure 2.8. When using CD, the molecules are freely suspended in solution and it is information about the structure of the protein that is obtained. DNA can be studied in the same way but that enquires higher concentrations or cuvettes of larger volumes to keep the noise low. In LD, only the signals from molecules that can be aligned, such as DNA, are detected and the molecules are therefore not freely suspended but instead aligned by some external force [39].

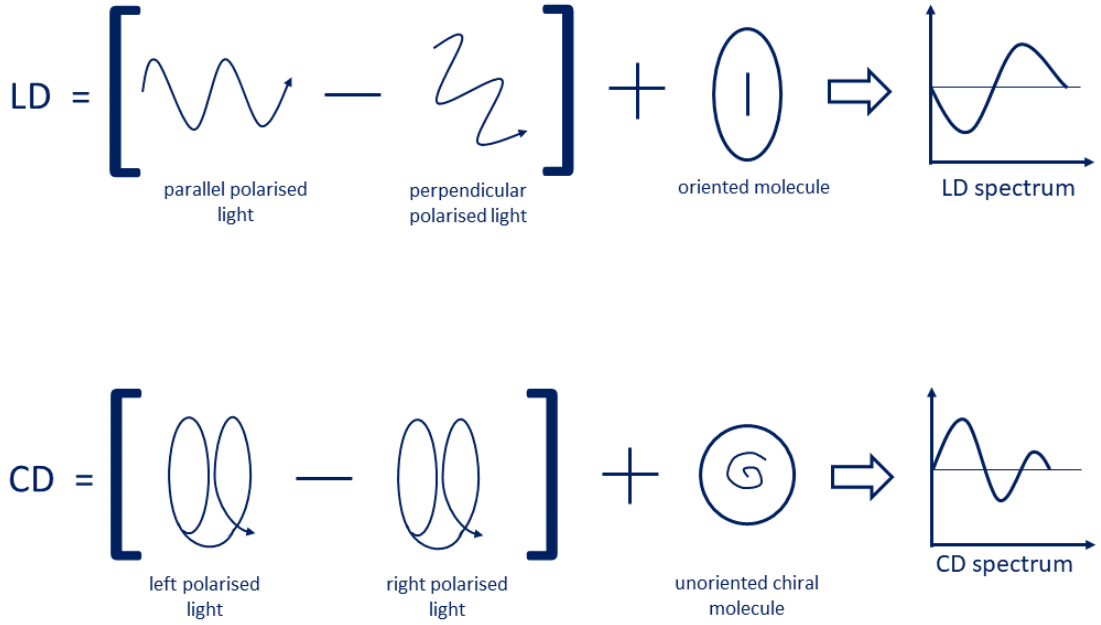

Figure 2.8: Schematic illustration of the theory behind LD and CD. LD detects the difference in absorption between parallel polarised and perpendicular polarised light in a sample of oriented molecules. CD detects the difference in absorption between left and right polarised light in a sample of unoriented molecules [40].

2.5.1.1 Circular dichroism

CD is an analytic tool used for rapid determination of the secondary structure and configuration of optically active molecules. The CD method analyses the absorption of polarised light that has passed through a sample, that is why only chiral and optically active molecules can be determined with CD [41]. Both proteins and DNA are suitable molecules for CD measurements due to the presence of chirality. In CD proteins absorb light within the 190-230 nm range and DNA within the 180-300 nm range [42, 43]. The most common application of protein CD is to determine whether an expressed and purified protein is folded, how it interacts with other molecules or if a mutation affects its conformation or stability [43]. The secondary structures of molecules give rise to characteristic and specific CD signals, see Figure 2.9, which makes it possible to investigate and compare the changes in the structure of both DNA and proteins. The signal that is detected in CD is the difference in absorption between left- and right-handed light and it is referred to as ellipticity, θ, which is expressed in degrees [41].

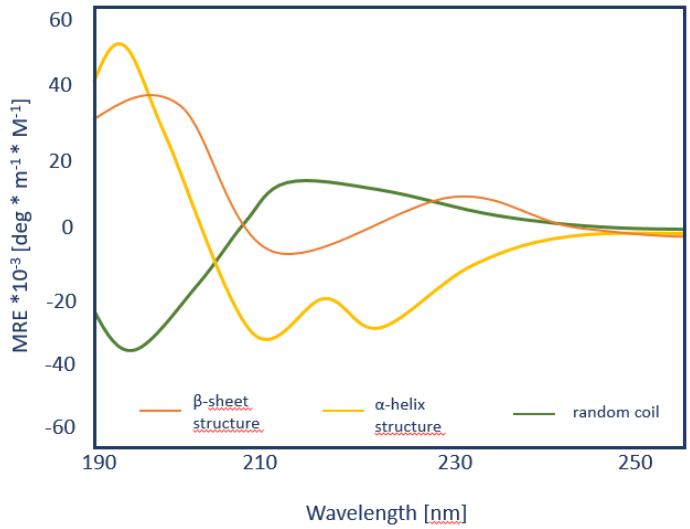

Figure 2.9: Graph illustrating characteristic and specific signals of CD for β-helix structure, α-helix structure and for unordered structure.

The electric field, E, of polarised light oscillates sinusoidally in a single plane. The sinusoidal wave can be visualised as the resultant of two vectors of equal length, which trace out circles in both right (E_R) and left (E_L) direction [40, 41]. When asymmetric molecules interact with polarised light, they may absorb right- and left-handed circularly polarised light to different extents and also have different indices of refraction for the two waves. The result is that the plane of the light wave is rotated and that the addition of the E_R and E_L vectors results in a vector that traces out an ellipse and the light is said to be elliptically polarised [43]. The result can henceforth be expressed in ΔE, the difference in absorbance of E_R and E_L but when the data is to be analysed, ellipticity is a more suitable unit. To be able to compare CD data, an expression of the ellipticity based on the molar concentration is in this case used, $[\theta]_{MRE}$.

$$[\theta]_{MRE} = \frac{\theta_{obs}}{10 * c * N * l} \tag{2.2}$$

Where θ_{obs} is the observed signal in degrees, c is the molar concentration, N is the number of peptide bonds (not applicable to DNA, for DNA N=1 is used) and l is the length of the cuvette in cm [43].

2.5.1.2 Linear dichroism

LD is also an electromagnetic spectroscopy method which uses the interactions between matter and light to obtain structural information about the molecules of interest [39, 44]. In the same way as CD, the LD method measures the difference in absorbance of two kinds of polarised light in a sample [45]. It is the difference in absorbance of parallel polarised light and perpendicular polarised light that is measured [40]. The changes in transmittance of the molecules give information about

the structure of the molecules in the sample. To be able to get visible results in LD, the molecules in the sample must somehow be macroscopically oriented. There are several ways to achieve orientation by stretching the molecules, the most common one is the Couette flow method [39, 40].

The Couette method aligns the macromolecules with shear flow, created by placing the sample between two rotating cylinders, see Figure 2.10. The magnitude of the LD signal depends on how well oriented the molecules are. When the Couette flow method is used, the rotation rate is what determines the orientation [40]. A high rotation rate without altering the molecule is desirable. When the orientation of the transition moments in the molecular coordinate framework is known, the signals from LD can give information about how the molecules are aligned in the sample.

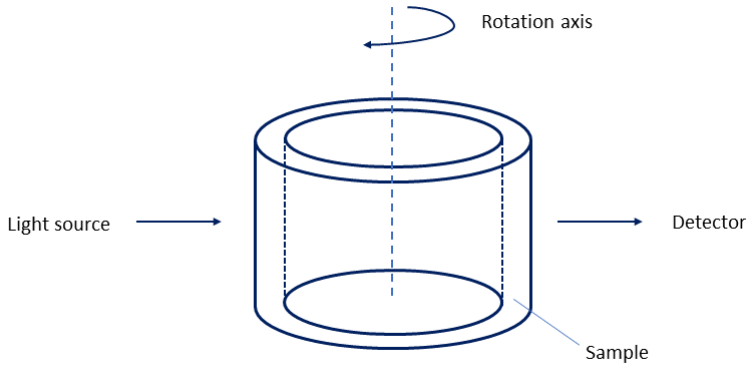

Figure 2.10: Schematic illustration of the Couette flow cell.

2.5.2 Fluorescence methods

In fluorescence spectroscopy, information is obtained from light emitted from molecules. Light can be described in many ways, for example as energy packages of photons where one package of energy, E, is proportional to its frequency of oscillation, as written in Equation 2.3 [46, 47].

$$E = hv = \frac{hc}{\lambda} \tag{2.3}$$

Where v is the frequency, λ the related wavelength, c the speed of light and h is Planck's constant. When molecules are irradiated with light their electrons can be affected by the light energy and thereby change their charge distribution. According to the Bohr frequency condition, Equation 2.4, the energy of light can be absorbed if it matches the energy gap, ΔE, between the initial energy state, E_1, and the excited energy state, E_2 [46, 47]. This excess energy is however quickly released through various processes, where the most common one is by releasing heat. There are also other ways, such as through fluorescence. When fluorescent molecules are exposed to light, their electrons will be excited and emit light of a lower wavelength than the one of the light source.

$$\Delta E = E_2 - E_1 = hv \tag{2.4}$$

The properties of fluorescent molecules can be used in several ways. In this project two fluorescence methods have been used; fluorescence spectroscopy and fluorescence microscopy. Fluorescence microscopes are light microscopes which create an image from the emitted fluorescence from the sample. The lamps used to irradiate the samples and excite the electrons, are high energy arc-discharge lamps due to their ability to generate a sufficient amount of photons [47].

2.5.2.1 Fluorescence spectroscopy: Thioflavin T assays

Fluorescence spectroscopy is a method widely used when studying amyloid proteins and how they aggregate. The method measures the emitted light from molecules that have been illuminated by a light source [48]. To make protein aggregates fluorescent, Thioflavin T (ThT) is commonly used, which is an amyloid fibril binding dye. The chemical structure of ThT is illustrated in Figure 2.11. ThT is a benzothiazole chemical that increases in fluorescence upon binding to large protein aggregates but not smaller ones such as oligomers [49, 50]. There is no known correlation between the intensity of the emitted light and the concentration of aggregated protein.

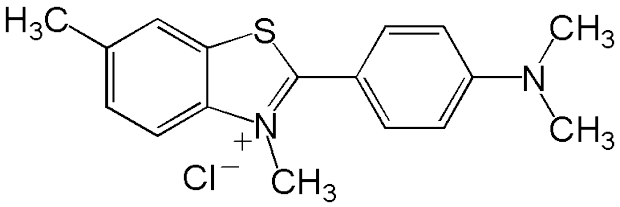

Figure 2.11: Chemical structure of the fluorescent dye Thioflavin T, generated in *ChemDraw Ultra 12.0*.

2.5.2.2 Fluorescence microscopy: Nanofluidic channels

Nanofluidic channels (NC) are used to visualise single DNA molecules by using fluorescence microscopy. Visualising single DNA molecules is an important method in order to understand the behaviour of DNA molecules, such as their replication, transcription and recombination [51]. The use of NC for this purpose has been an established method for several years. However, some modifications of the method have been made, which allow for investigations of DNA-protein interactions [52]. The interactions can be recorded to be studied and compared between samples to see structural changes. Interactions of DNA with oligomers as well as fibrils can be studied with this technique.

The main advantage of studying DNA-protein interactions using NC is that the studies are implemented on the molecules freely suspended in solution. This means a minimum of factors affecting or disturbing the configuration of the DNA molecules, which has been problematic in previous methods [52]. The method also gives a unique opportunity to study the molecules at a single molecule level while freely

suspended. To get clear images of the DNA, the molecules are stained with the fluorescence cyanine dye YOYO-1 (YOYO). The chemical structure of YOYO is illustrated in Figure 2.12. The binding between DNA and YOYO has an established effect on the properties of DNA. YOYO is a highly positively charged molecule and therefore reduces the negative charge of DNA upon binding. Each intercalated YOYO molecule increases the length of the DNA molecule with 0.51 nm and reduces the twist of the helical structure by about 24 degrees.

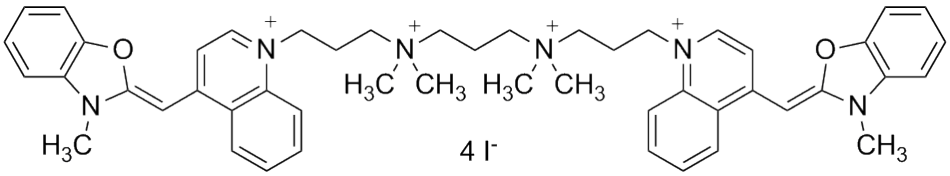

Figure 2.12: Chemical structure of the fluorescent dye YOYO-1, generated in *ChemDraw Ultra 12.0*.

The channels of nanosize used in NC are connected in a small chip, as can be seen in Figure 2.13. The chip is then connected to a plate which in turn is connected to a nitrogen flow, regulating the pressure. The sample is added to a well in the plate and pushed, molecule by molecule, into the nanochannels via the microchannels. Figure 2.14 shows a DNA molecule that was pushed through a nano-sized channel. It is important to coat the channels with a material that will not affect or bind the DNA or protein [51, 52]. This can cause problems since DNA is generally a negative molecule and protein a positively charged one and it is difficult to find a material that will not attract either of these. To get the benefits from NC, the DNA and protein must flow unhindered in the channels. It is therefore not only an issue of opposite charge attraction but also a size issue, the coating material must be small enough not to clog the channels [53]. Lately, lipids have been used to coat the surface of NC. The idea to use lipids as a protecting layer comes from the living cell which often is built of a lipid bilayer which effectively resists all non-specific bindings [54].

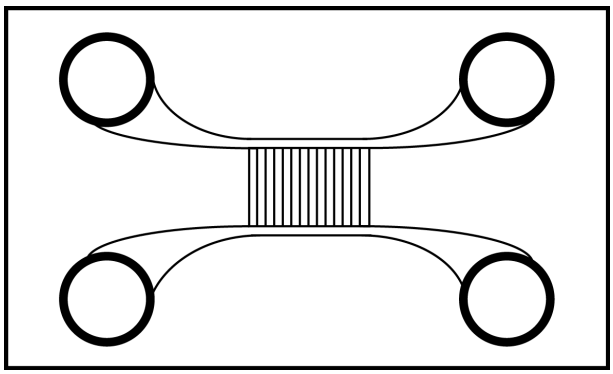

Figure 2.13: Schematic image of a NC chip, visualising 4 wells for sample addition and 2 micro channels leading to the nanochannel area in the centre.

Figure 2.14: Image of a DNA molecule stained with YOYO in a nanochannel, taken with a fluorescence microscopy.

2.5.3 Atomic force microscopy

Atomic force microscopy (AFM) is a analysis method used to obtain information about a surface or a molecule. AFM provides high-resolution images and information about the topography of the sample, an example of an AFM image is shown in Figure 2.15 [55]. To the right of the image, a height scale is located, showing what height corresponds to the colours of the image.

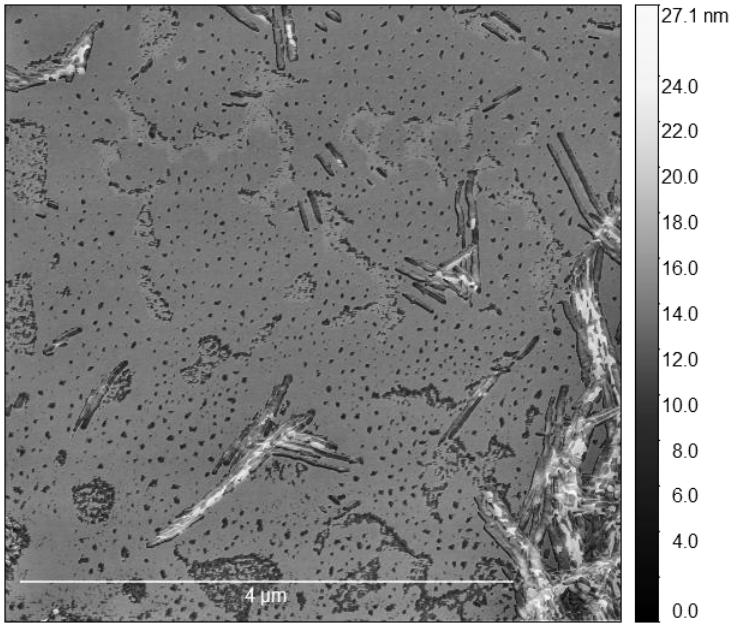

Figure 2.15: AFM image of tangled αS fibrils on Mica surface.

Tapping AFM uses a nanometer-sized probing tip which is located in close proximity above the surface of a sample [56]. The probing tip sends information based on the attracting or repulsing forces acting within the contact area to a detector. An electric platform, on which the sample is placed, controls the motion of the sample and maintains the desired distance between the probe and the sample surface. When a specific molecule from a liquid sample, such as DNA, is to be studied one method is to dry the sample on a surface. Two types of surfaces commonly used for DNA-protein studies are silica or Mica surfaces [57]. Mica is a phyllosilicates material which can be used for both coated and bare DNA while silica surfaces can only be used for studying protein-coated DNA [58].

3
Methods

This chapter contains specific information about the compounds and methodology used in the experimental work of this thesis. All samples of αS used in the laboratory work were prepared at Chalmers by Ranjeet Kumar.

3.1 Preparation of protein and DNA

Throughout the project, fresh stocks of both DNA and αS were necessary. Monomeric αS was provided by GFC of samples of αS, while λ-DNA, 10k DNA and 1k DNA were bought as premade solutions from *Thermo Scientific*^{TM}. Stock solutions of ctDNA were prepared as described in this section.

3.1.1 Purifying α-synuclein with gel filtration chromatography

To ensure a monomeric solution of αS, GFC purification was performed on samples of αS synthesised according to the method described in; [59]. Stock solutions (1 ml) of αS with a concentration of 2 mg/ml were used and concentrated down to a volume of 600 μl using *Amicon® Ultra 0,5 ml* centrifuge filter. The size of the filter used was 10 kDa and the solution was centrifuged for 3 minutes at a speed of 12 g. The protein solution of 600 μl was then injected into a *S75 Superdex* gel column, connected to *ÄKTApurifier*^{TM} at 4 °C. A buffer, *Tris-EDTA buffer solution* (TE-buffer) with a pH of 7.4, purchased from *Sigma-Aldrich*, was used as mobile phase. The TE-buffer contains 10 mM Tris-HCl and 1 mM EDTA. EDTA is a good binder of metal ions and therefore prevents damage of biomolecules sensitive to metal binding [60].

The absorbance of the eluate was measured and put, 1 ml per fraction, in sample tubes. The fractions containing monomeric αS were selected according to the absorbance spectra at 280 nm. The concentration of the protein was determined with *Lambda Bio+* UV/vis spectrophotometer using a 1 cm quartz glass cuvette with 1 ml sample, 5960 $M^{-1}cm^{-1}$ was used as the molar extinction coefficient for αS. When a higher concentration was needed, the sample was again concentrated using *Amicon® Ultra 0.5 ml* centrifuge filter. The protein was then stored at 4°C if it was to be used the same day. If the protein had to be stored more than 12 hours it was flash frozen with liquid nitrogen and stored at -80°C to avoid aggregation.

3.1.2 Preparation of DNA stock solution

The ctDNA used in the laboratory work was purchased from *Sigma-Aldrich* and stored at -18°C. To prepare stock solutions of ctDNA approximately 0.002 g of dry ctDNA were used. 5 ml of TE-buffer was added to the DNA and the solution was carefully mixed until the DNA was dissolved. The tube was then fixed on a rocker shaker and left for gentle mixing at 4°C during 24 hours to ensure that the DNA was completely dissolved. 1 ml of the DNA solution was then put into a 1 cm quartz glass cuvette and the absorbance at 260 nm was measured to obtain the stock concentration, 13200 M $bp^{-1}cm^{-1}$ was used as the molar extinction coefficient for DNA. The DNA was then stored long-term at -18°C and short-term, maximum of one week, at 4°C to ensure a high quality of the DNA molecules.

3.2 Circular dichroism experiments

CD measurements were performed with a *Jasco-810* CD spectrometer at room temperature, using a 0.1 cm quartz glass cuvette with a sample volume of 300 μl. The wavelengths were measured from from 195 to 300 nm, with several accumulations, giving a mean value, which was used as raw data. Before each series of samples, a blank sample of TE-buffer was measured to create a baseline. Measurements were first performed on αS and ctDNA alone, to obtain reference data. The experiments were then done by having a constant concentration of αS (12 μM) and different concentrations of ctDNA or by titration of DNA into a sample of αS (12 μM). The ratios (αS:ctDNA bp) measured were: 1:0, 1:0.5, 1:2, 1:5, 1:8 and 1:12. More detailed information concerning the preparation of CD samples can be found in Appendix A. All samples were prepared right before the measurements and in between each measurement the cuvette was washed with distilled water, ethanol and TE-buffer.

The *Jasco-810* CD spectrometer was connected to a computer where *Spectra Manager*^{TM} from *Jasco*$^{®}$ was used to control the measurements. The data obtained was analysed and recalculated into molar ellipticity with *Spectra Analysis*^{TM}. The results from protein-DNA experiments were modified by removing the signals created by the ctDNA. This was done to visualise possible structural changes in αS. The processed data was plotted in *Excel* against the wavelengths.

3.3 Linear dichroism experiments

LD measurements were performed on a *Chirascan*$^{®}$ spectrometer at room temperature, using a Couette flow cell with a sample volume of approximately 1.5 ml and a cuvette path length of 0.1 cm. Samples used in the cell contained ctDNA (10 μM bp), αS and for some experiments, YOYO (0.2 μM) or NaCl (150 μM). The amount of αS was varied into the following ratios (ctDNA bp:αS): 1:0, 1:0.04, 1:1, 1:2 and 1:4. Further information about the sample preparation can be found in Appendix B. The wavelength range measured in the experiments were 195 to 400 nm and the samples were incubated for 1 hour and for 24 hours after preparation, at 4°C. The

incubation was done to investigate if time affects the DNA structure. The rotation rates used were 600 rpm, 800 rpm and 1000 rpm, where 1000 rpm (3100 s^{-1}) was chosen as the optimal rotation rate since it gave rise to clear LD signals and no breaking of the DNA molecules was detected. All samples were also measured without rotation which was used as a baseline and subtracted from the data. The baseline corrected LD signals were plotted in *Excel* against the wavelengths.

3.4 Atomic force microscopy experiments

Samples of 1k DNA and 10k DNA (5 μM bp), αS and TE-buffer were prepared in molar ratios (ctDNA bp:αS) of 1:0, 1:0.02, 1:0.2 and 1:2. More details regarding sample preparation can be found in Appendix C. The samples were incubated for 4 hours at 4°C. Mica and silica wafers were put on sample holders using tape. Approximately 20 μl of each sample was pipetted onto the surfaces, making doublets of each sample. Samples containing only TE-buffer and DNA were put on Mica surfaces and samples containing DNA, protein and TE-buffer were put on silica surfaces. The liquid samples were left on the surfaces for 3 minutes to get the DNA to absorb onto the surfaces. The liquid samples were then removed and the surfaces were washed with distilled water to remove any excess sample. The washing process changed during the project in order to find the most effective way to remove the buffer without endanger the absorption of the DNA molecules. To wash the samples, the wafers were put into water briefly, left in water for 5 minutes or rinsed with 1000 μl of water. The water left on the sample after washing was first removed carefully with a paper tissue and then dried off with a gentle flow of nitrogen gas.

The dry samples were studied using *NT-MTD*^{TM} force microscopy with a golden silicon probe *NSG01*. *Nova*^{TM} was the software used to obtain images of the samples. Additionally, an extern software, *Gwyddion*^{TM}, was used to analyse the images.

3.5 Thioflavin T assay

To study the aggregation of αS, fluorescence spectroscopy was used with ThT as a fluorescence amyloid-binding dye. The measurements were done in *FLOUstart*® *Omega* plate reader with a 96 well plate. The temperature was set to 37 °C and the reading time to 160 hours with shaking. The samples (50 μl) that were studied contained ctDNA, αS (50 μM), NaCl (150 μM), ThT (13.5 μM) and TE-buffer. The ratios of αS:ctDNA bp studied were: 1:0, 1:0.01, 1:0.25, 1:0.5 and 1:1. The samples were prepared and added into the wells, in every well there was also a glass bead put to further increase the agitation. The wells on the edges of the plate were not used in order to avoid overheating and evaporation of the samples. Apart from the samples of DNA and protein, control samples were measured in the wells as well. The controls were made without αS , see Appendix C for complementary data about ThT assay experiments. The aggregation experiment was repeated once. The control samples ensured that ThT does not emit light when unbound and that all

emitted light is due to the presence of amyloid fibrils. After the ThT assay was done, the samples were removed from the wells and put on Mica plates to be studied by AFM microscopy. The samples were left on the Mica surfaces for 10 minutes to let the fibrils and DNA molecules adsorb onto the Mica surface and was then washed three times with distilled water.

3.6 Nanofluidic channel experiments

Samples with a volume of 20 μl, containing λ-DNA (5 μM bp), αS, TE-buffer and YOYO (0.2 μM) were prepared and incubated for 4 hours in darkness at 4 °C. The ratios of ctDNA:αS in the samples were: 1:0, 1:0.2, 1:1, 1:3, 1:8, see Appendix E for more information about the sample preparation. A NC chip was during the time coated with lipid vesicles by flushing the lipid vesicles through the chip. Two different sizes of channels were used for studying the molecules, 150x100 nm^2 and 150x700 nm^2. All gas bubbles were removed from within the chip before the experiment was started by flushing TE-buffer through the channels. β-Mercaptoethanol (BME) was added into the sample, to increase the stability of the DNA molecules. 15 μl of the DNA and protein samples were added into the chip and flushed through the microchannels into the nanochannels. The movement of DNA was studied with a *Zeiss AxioObserver.ZI epi* fluorescence microscopy which was equipped with a FITC filter, making it possible to see the fluorescent molecules. The lamp used to excite the molecules was a halogen lamp of *Mercury Short Arc HBO®*. To record the movements and obtain data, a Photometric Evolve Electron Multiplying Charge Coupled Device camera was used.

To analyse the data from the NC experiments an established *MATLAB* script was used, the script identifies where in the images the DNA molecules are located. From their location, a cymograph was created by stacking the images on top of each other and the size of the DNA molecules was determined. The extension of the molecules was plotted against the fraction of molecules an visualised in histograms to show the effect of αS on the DNA extension.

4

Results and discussion

The main results obtained in the laboratory work are presented and discussed in this chapter. Supplementary information is presented in Appendix A-E. The results are arranged by information related to interaction studies in bulk phase or at the single molecule level.

4.1 Interactions between α-synuclein and DNA in bulk phase

This section contains the results from LD and CD experiments. The aim is to obtain information about the structural changes within the secondary structure of the molecules, due to potential interactions between αS and DNA in the bulk phase.

4.1.1 Linear dichroism results

LD experiments of αS and ctDNA samples were carried out 1 hour after sample preparation as well as after 24 hours of incubation. The results are presented in Figure 4.1 and in Appendix B, Section B.2. The ctDNA molecules are long enough to be oriented in the shear flow of the Couette cell with the helix axis parallel to the flow direction, as indicated by the negative LD peak at 260 nm that results from the perpendicularly oriented DNA bases. When αS is added to the sample, no significant changes are observed in the negative peak at 260 nm, suggesting that the DNA structure is not affected. An increase in the LD signal can be seen around 210 nm, which could indicate that αS binds to DNA, since the amide groups in proteins give rise to the transition observed in the far UV region (180-240 nm). In LD only aligned molecules are detected. Protein molecules are too small to be aligned and detected on their own making protein-DNA interaction a possible explanation to the increase in LD signal at 210 nm. Using LD, nothing can be said about potential structural changes occurring in αS due to interaction with DNA. The secondary structure of αS was investigated by CD experiments, which are presented in the next section. Increased incubation time seems to have no apparent effect on the LD spectra.

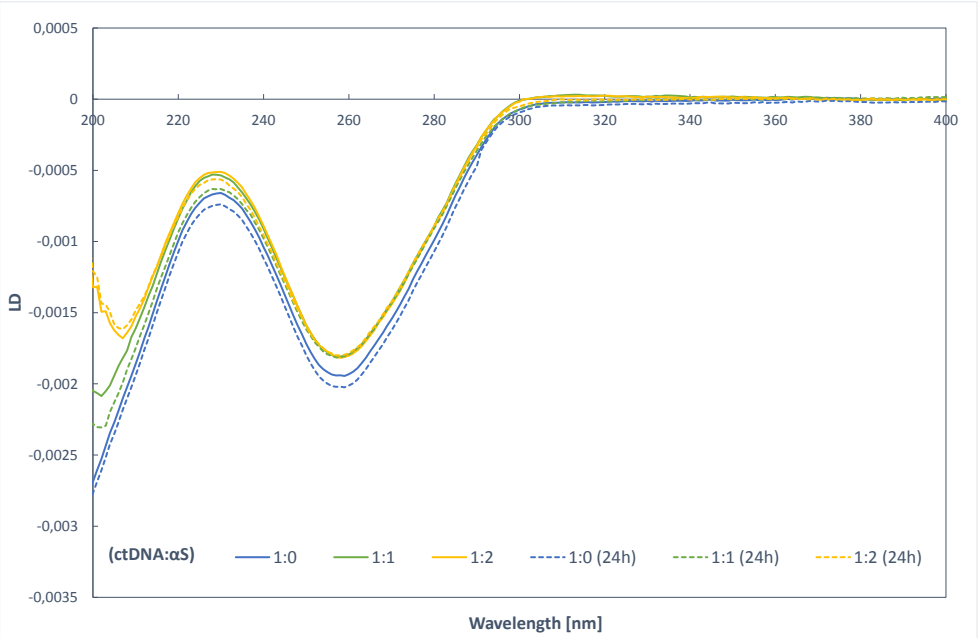

Figure 4.1: LD spectra of ctDNA (10 μM bp) with various concentrations of αS. Samples were incubated for 1 hour and 24 hours after preparation. The increase of signal at around 210 nm for samples with DNA and αS suggests protein-DNA interactions.

LD experiments with YOYO and NaCl were also carried out, mostly to investigate if these chemicals affected the DNA structure. However, these experiments showed no significant differences when compared to the samples without the dye or NaCl, apart from the fact that DNA gets less aligned in the presence of NaCl, see Section B.2.

4.1.2 Circular dichroism results

Figure 4.2 shows the CD spectra of ctDNA alone in TE-buffer at various concentrations. The overall shape of the curves is comparable with literature data where the local maxima and minima of the spectra can be associated to the nucleotides of DNA [40]. The peak around 275 nm is due to content of C and T, the local minima around 250 nm is due to G content and the rise at 200 nm is due to G and A content [40].

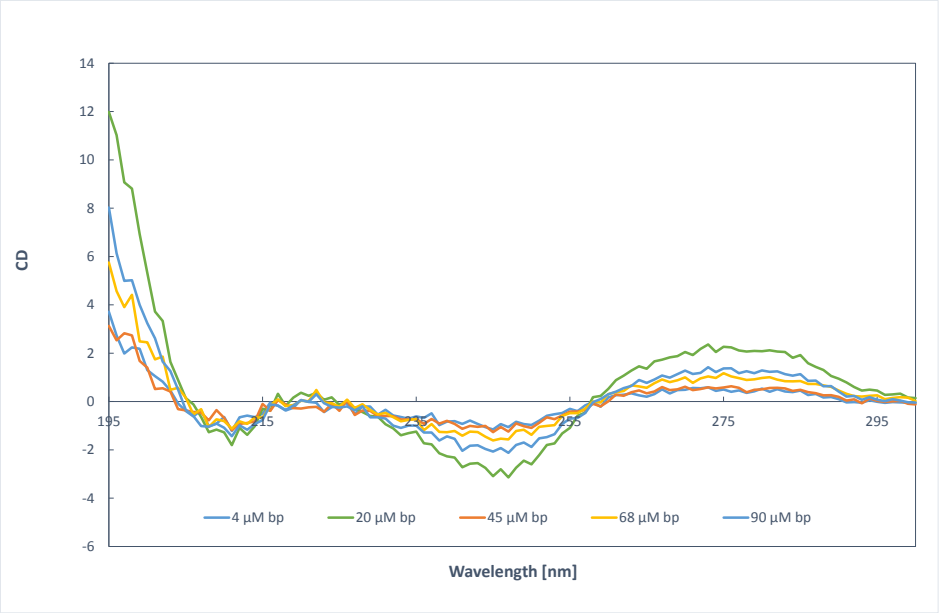

Figure 4.2: CD spectra of ctDNA in TE-buffer showing its characteristic shape. The local maxima and minima of the spectrum can be associated to the nucleotides in DNA.

Figure 4.3 presents the spectra from CD experiments of αS (12 μM) mixed with ctDNA. The sample of αS alone shows a negative band at around 200 nm, which is a typical CD spectrum of unordered secondary structure. As can be seen, there are no distinct changes in the spectra of the samples with DNA. The uniform spectra indicate that there are no structural changes in αS. In the 195-210 nm region, there are some differences between the samples, possible due to measurement noise. At low wavelengths and high concentrations of protein and DNA, noise is a reasonable explanation for signals behaving in this matter, the high tension voltage was, however, still within acceptable values. Secondary structural features of proteins are seen in the 210-230 nm region as well as in the 195-210 nm region. The spectra do therefore not indicate any changes in structure of the protein upon binding to DNA.

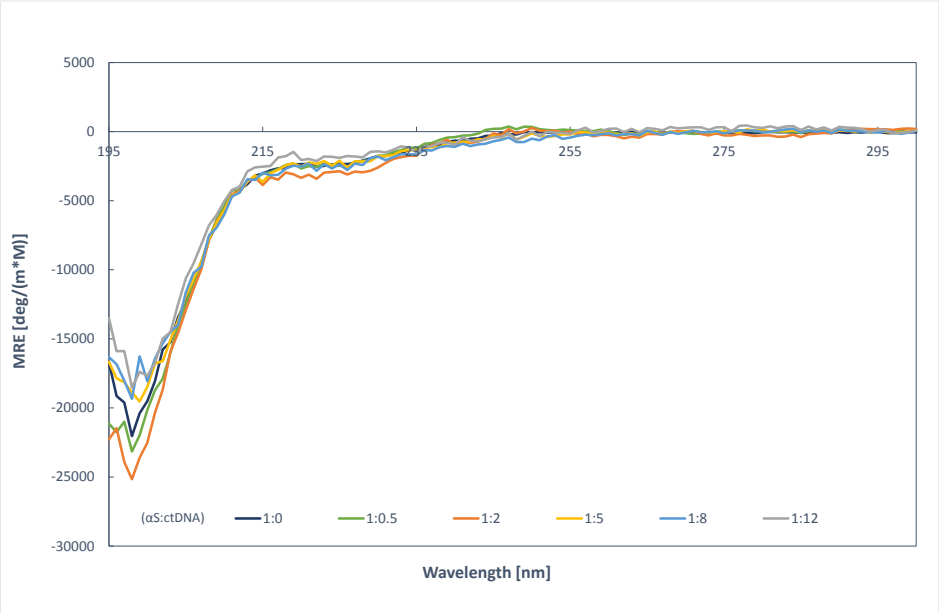

Figure 4.3: CD spectra of αS (10 μM) titrated ctDNA in TE-buffer.

The samples investigated with CD had a constant concentration of protein and varying concentrations of DNA, incubation times of only a few minutes and a measurement temperature set to room temperature. All these parameters can be modified to study the interaction of αS with DNA at different conditions. In future experiments it would also be of interest to change the protein concentration and investigate the DNA structure. Varying the protein concentration could lead to CD spectra with less noise and a possibility of more detailed observations of slight changes in the spectra. Previous research has shown changes in the structure of supercoiled DNA induced by αS [29]. According to their CD measurements, there were strong indications of binding, causing a conformational change from the B-form of DNA to an altered B-form. In contrast, LD measurements of ctDNA showed that there are no significant changes in the DNA structure in the presence of αS. This observation points out that the protein-DNA interaction could well depend on the ratios and/or DNA structure and sequence.

In future experiments it would also be of interest to study a mutant of αS where the N-terminal domain has been modified. It is well studied that when αS interacts with and binds to micelles it forms an α-helical structure. It is the positively charged N-terminal domain of αS that interacts and get a more ordered structure.

4.2 Interactions between α-synuclein and DNA at a single molecule level

In this section the results from NC and AFM experiments are described. The aim is to obtain information about the behaviour of the protein-DNA interactions at a single molecule level.

4.2.1 Nanofluidic channel results

With NC it was possible to obtain images of single DNA molecules pushed through nano-sized channels. Figure 4.4 shows a montage of fluorescence images of five λ-DNA molecules being stretched by the nanochannels. The concentration of αS used is written next to respective DNA molecule. The image shows how the length of the DNA molecules increases with increased protein concentration. The increased molecule length is due to less folding of the DNA, achieved by interactions with αS. An explanation for this can be that the positively charged parts of αS bind to the negatively charged phosphate groups of DNA and by that increasing the coverage of the DNA molecule, with increased concentration of αS. When the DNA molecule gets coated with protein it loses its ability to fold itself and acquires a stiffer configuration where an increased extension is observed.

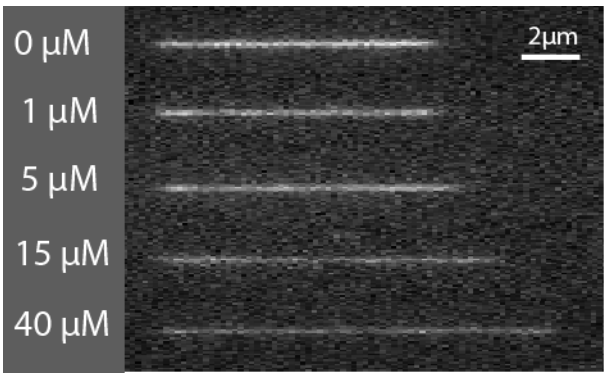

Figure 4.4: Image of λ-DNA (5 μM bp) with αS (0 μM, 1 μM, 5 μM, 15 μM and 40 μM) in 150x100 nm channels. An increase in length of the DNA molecule can be observed with increasing concentrations of αS.

The numbers of molecules and their length were determined and visualised in histograms, which are displayed in Figure 4.5. Here, the same conclusion of increased extension is showing for channels with a size of 150x100 nm^2. The extension of the DNA molecule is increased with increasing concentrations of αS. The persistence length, which is a mechanical property quantifying the stiffness of a long molecule, was studied as well. This was done by Sriram KK and Kevin D Dorfman at the University of Minnesota. The investigation of the persistence length of the DNA

molecules determined an increase in length from 70 nm to 90 nm when incubated with high concentrations of αS.

The histograms to the right of Figure 4.5 were obtained using channels of 150x700 nm^2, and do not show the trend of increased DNA extension as pronounced as in the smaller sized channels. At αS concentrations of 40 μM, a clear increase in the length of DNA is observed even in the wide channels. The wide channels of 700 nm allow the DNA to be loosely folded even when coated with protein, until it is majorly coated at high concentrations of protein. The reason for the extension of DNA after interaction with protein is probably due to a stiffer configuration created by repulsive charges caused by αS.

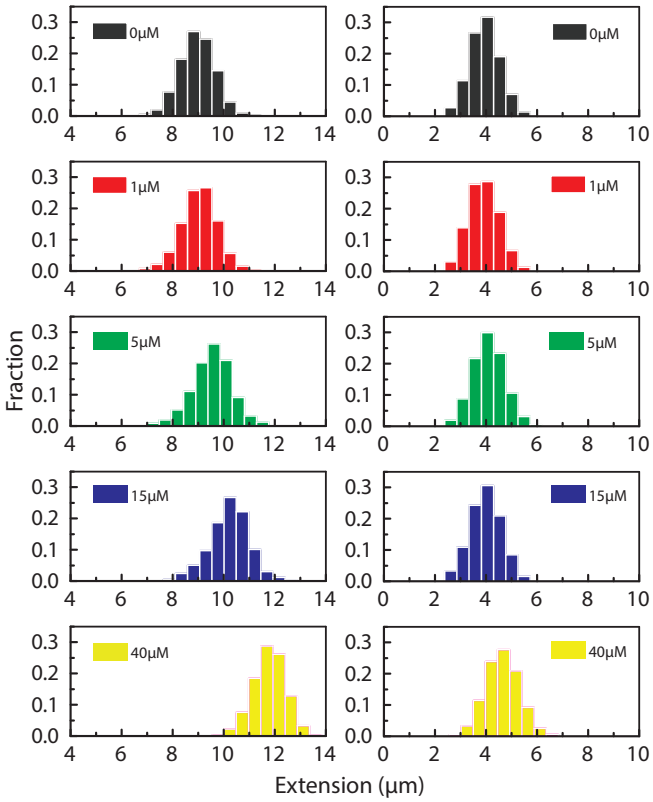

Figure 4.5: Histograms of λ-DNA (5 μM bp) with αS (0 μM, 1 μM, 5 μM, 15 μM and 40 μM) in 150x100 nm^2 channels to the left and 150x700 nm^2 channels to the right. An increase in length of the DNA molecule can be observed with an increasing concentration of αS.

4.2.2 Atomic force microscopy results

Images were taken of dried samples of αS with 1k DNA and 10k DNA using tapping mode AFM. The samples were dried on a surface of silica or Mica. Silica only adsorbs DNA molecules that have interacted with αS, making it a good control to support the results from NC experiments. An AFM image of bare 1k DNA is shown in Figure 4.6. The molecules have a uniform morphology and an even height of 0.5 nm.

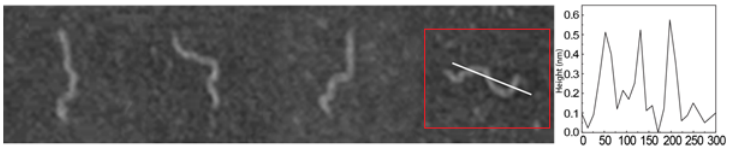

Figure 4.6: AFM images of 1k DNA (5 μM bp), dried on a surface of Mica, to the right, a graph showing the height of the marked DNA molecule, the height was estimated to be approximately 0.5 nm.

In Figure 4.7, samples of DNA and αS adsorbed on silica wafers are presented. 1k DNA is seen as small lines on the surface with clusters of αS bound to them, resulting in a non uniform shape of the DNA molecule. When studying the AFM images it was observed that at low concentrations of αS (1:0.02), the DNA molecules got repeating clusters of protein bound to them. In Figure 4.7 D, a graph of the height of a DNA molecule is displayed. The height is not the same along the molecule, which is different from the bare DNA molecule. A difference between 1 nm and 2 nm is observed confirming the uneven morphology. This is an increase in height of 1.5 nm compared to bare DNA. That αS binds to DNA in clusters suggests that there are favourable specific sequences on the DNA molecule where αS binds with a higher affinity. There have been studies showing that the interaction occurs preferably with GC-box-like sequences of DNA. To further investigate this, modified DNA sequences could be used together with single molecule studies and isothermal titration calorimetry, which is a method to determine enthalpy of the binding reaction and estimate the association constant.

The behaviour of αS binding to DNA in clusters was not possible to observe in images from NC experiments. In images of the DNA molecules in the nanochannels, taken with fluorescence microscopy, the coating of αS looked evenly distributed on the molecule. This is an interesting observation that could be explained by a competition of binding sites between YOYO and αS or the difference in GC-content in ctDNA and λ-DNA. More likely is however that the difference in morphology between NC and AFM images is solely due the two methods having different resolutions.

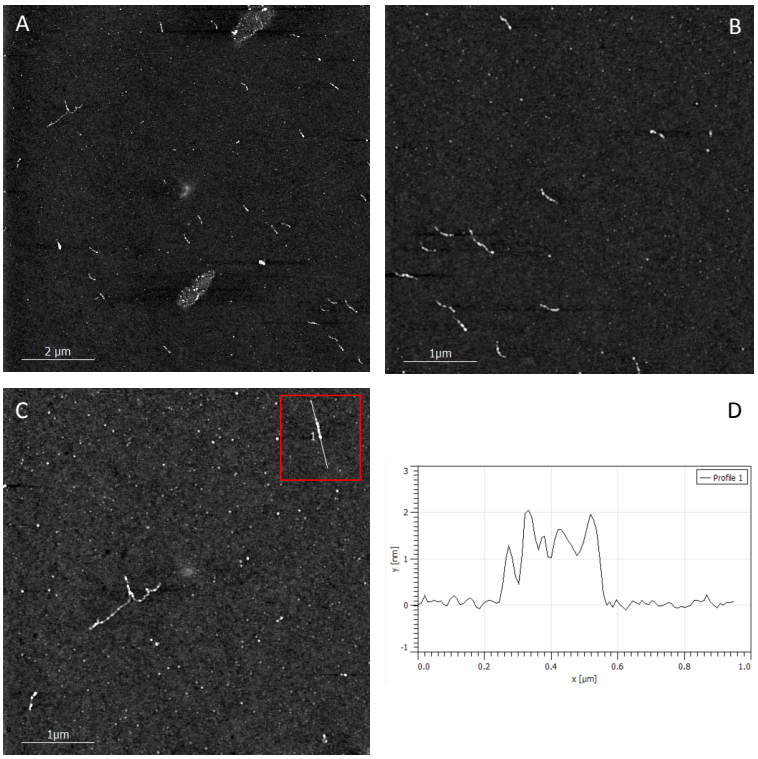

Figure 4.7: AFM images of sample of αS (0.1 μM) and 1k DNA (5 μM bp), dried on a surface of silica. In image A, several DNA molecules coated with αS are observed. Image B and C are zoomed in areas of image A. Image D shows a graph with the height of the marked DNA molecule in image C; the height was estimated to approximately 2 nm.

4.3 Aggregation studies of α-synuclein in the presence of DNA

Aggregation studies were performed to investigate if the presence of DNA affects the aggregation of αS. The experiment was done twice, with varying results, making it necessary to repeat this experiment several times to be able to draw any conclusions. In Figure 4.8, preliminary results from an aggregation study are presented, from which also AFM samples were taken, which are displayed in Figure 4.9. In Appendix D all supplementary data and results are presented.

The obtained graph displays the fluorescence intensities from samples of three concentrations of ctDNA against time expressed in hours. As can be seen, there is no clear trend in the data with regards to the DNA concentration, instead, all samples seem to have a lag time of about 10 hours and reach a plateau shortly after. The previous results showed a similar lack of trends but also with a lag phase of 10 hours. It could be that DNA takes no part in the aggregation of αS in this experiments. The αS will aggregate in this time span solely by the help of NaCl and the glass beads.

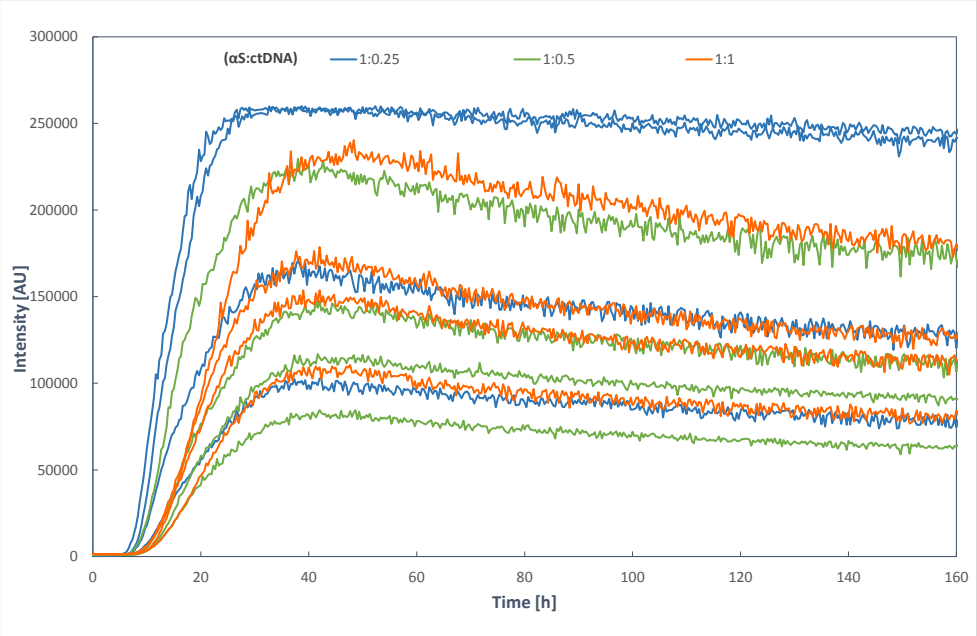

Figure 4.8: Aggregation study using ThT assay with samples of αS (50 μM) together with ctDNA (12,5 μM bp, 25 μM bp and 50 μM bp) and NaCl (150 μM).

To further investigate if any differences could be found between the aggregation samples, AFM was performed. The images of αS samples containing 12.5 μM bp, 25 μM bp and 50 μM bp ctDNA are displayed in Figure 4.9. The images show the fully aggregated state of αS in fibrils for all concentrations of DNA. It is hard to determine if there are any differences between the samples or if DNA interacts with the fibrils. The DNA molecules should be visible on the images even if they take no part in the aggregation. However, due to their small size of 0.5 nm, compared to the ∼20 nm size of the fibrils, they will be hard to localise and identify.

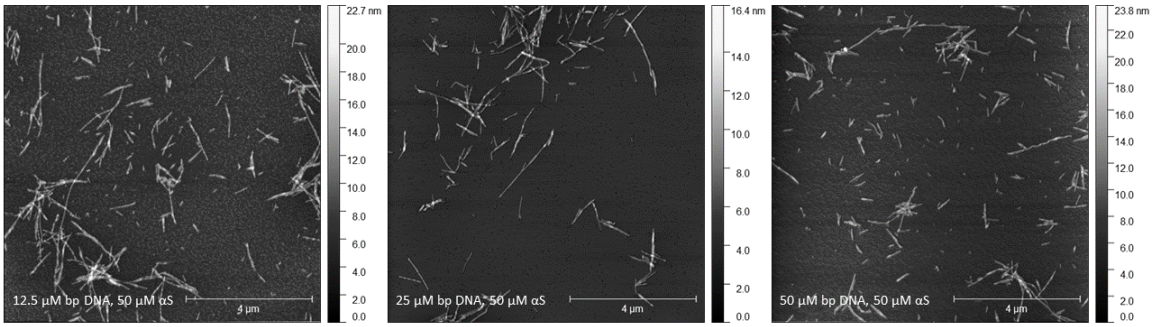

Figure 4.9: AFM images of αS samples after incubation at 37°C with different ctDNA concentrations, deposited on Mica.

5
Conclusion

Interactions between DNA and αS could be observed in results obtained from LD, NC and AFM experiments. These interactions, which are believed to be partly of an electrostatic character, can be studied in both bulk phase and at a single molecule level. AFM images showed signs of favourable binding sites on the DNA molecules, which would be of interest to study in future experiments using modified DNA molecules. The suggestion that the binding of αS to DNA occurs favourably to the GC-box-like sequences could then be investigated. The trend of αS binding to specific parts of the DNA molecules was not observed in images obtained from NC experiments, most likely due to an image resolution too low to detect them.

In experiments using CD, samples of αS and ctDNA were investigated to determine secondary structural changes in αS, induced by DNA. According to these result, there were no indications of secondary structural changes of αS. However, an increased stiffness of the DNA molecules was observed in NC experiments. The increased stiffness caused by αS results in an extension of the molecule length. That αS interacts with DNA and affects its configuration could be of great importance in research in the field of amyloid diseases such as PD, since αS has been reported to be present in the nucleus where it could act as a transcription modulator. There have also been studies showing that αS facilitates double-stranded DNA breaks upon oxidative stress. To study potential breaking of DNA caused by αS is an interesting next step in the understanding of DNA-αS interactions.

In summation, the thesis was able to investigate the questions issued in the aim. The project has shown that αS and DNA interact with each other without indications of secondary structural changes but with an increased DNA stiffness. Furthermore, indications of favourable αS binding sites were observed on the DNA molecules.

References

(1) Chaudhuri, K. R.; Clough, C. G.; Sethi, K. D., *Fast Facts: Parkinson's Disease*; Health Press Limited Abingdon: 2011.

(2) Stefanis, L. α-Synuclein in Parkinson's disease. *Cold Spring Harbor perspectives in medicine* **2012**, *2*, a009399.

(3) NIDA, Q. Dopamine pathways., [Online; accessed 25-April-2018], 2012.

(4) Breydo, L.; Wu, J. W.; Uversky, V. N. α-Synuclein misfolding and Parkinson's disease. *Biochimica et Biophysica Acta (BBA)-Molecular Basis of Disease* **2012**, *1822*, 261–285.

(5) Kalia, L. V.; Lang, A. E. Parkinson's disease. *The Lancet* **2015**, *386*, Copyright - Copyright Elsevier Limited Aug 29, 2015; Last updated - 2017-11-22; CODEN - LANCAO, 896–912.

(6) Maroteaux, L.; Campanelli, J. T.; Scheller, R. H. Synuclein: a neuron-specific protein localized to the nucleus and presynaptic nerve terminal. *Journal of Neuroscience* **1988**, *8*, 2804–2815.

(7) Polymeropoulos, M. H.; Lavedan, C.; Leroy, E.; Ide, S. E.; Dehejia, A.; Dutra, A.; Pike, B.; Root, H.; Rubenstein, J.; Boyer, R., et al. Mutation in the α-synuclein gene identified in families with Parkinson's disease. *science* **1997**, *276*, 2045–2047.

(8) Surguchev, A. A.; Surguchov, A. Synucleins and Gene Expression: Ramblers in a Crowd or Cops Regulating Traffic? *Frontiers in molecular neuroscience* **2017**, *10*, 224.

(9) Vasquez, V.; Mitra, J.; Hegde, P. M.; Pandey, A.; Sengupta, S.; Mitra, S.; Rao, K.; Hegde, M. L. Chromatin-Bound Oxidized α-Synuclein Causes Strand Breaks in Neuronal Genomes in in vitro Models of Parkinson's Disease. *Journal of Alzheimer's Disease* **2017**, *60*, S133–S150.

(10) Emamzadeh, F. N. Alpha-synuclein structure, functions, and interactions. *Journal of research in medical sciences: the official journal of Isfahan University of Medical Sciences* **2016**, *21*.

(11) Hegde, M. L.; Rao, K. DNA induces folding in α-synuclein: understanding the mechanism using chaperone property of osmolytes. *Archives of biochemistry and biophysics* **2007**, *464*, 57–69.

(12) Vasudevaraju, P; Guerrero, E.; Hegde, M. L.; Collen, T.; Britton, G. B.; Rao, K. New evidence on α-synuclein and Tau binding to conformation and sequence specific GC* rich DNA: relevance to neurological disorders. *Journal of pharmacy & bioallied sciences* **2012**, *4*, 112.

(13) Padmaraju, V.; Bhaskar, J. J.; Prasada Rao, U. J.; Salimath, P. V.; Rao, K. Role of advanced glycation on aggregation and DNA binding properties of α-synuclein. *Journal of Alzheimer's Disease* **2011**, *24*, 211–221.
(14) Sjöström, H.; Nordlund, S. Proteiner., [Online; accessed 14-May-2018], 2018.
(15) Buxbaum, E., *Fundamentals of protein structure and function*; Springer: 2007; Vol. 31.
(16) Commons, W. File:Figure 03 04 09.jpg — Wikimedia Commons, the free media repository., [Online; accessed 15-May-2018], 2017.
(17) Berezovsky, I. N.; Guarnera, E.; Zheng, Z. Basic units of protein structure, folding, and function. *Progress in biophysics and molecular biology* **2017**, *128*, 85–99.
(18) Ulrich, H.; Giovanni, M.; Giuseppe, V., *DNA Polymerases: Discovery, characterization and functions in cellular DNA transactions*; World Scientific: 2010.
(19) Sinden, R. R., *DNA structure and function*; Elsevier: 2012.
(20) Limited, G. R. DNA double helix., [Online; accessed 04-May-2018], 2016.
(21) Gibb, W.; Lees, A. The relevance of the Lewy body to the pathogenesis of idiopathic Parkinson's disease. *Journal of Neurology, Neurosurgery & Psychiatry* **1988**, *51*, 745–752.
(22) Masliah, E.; Rockenstein, E.; Veinbergs, I.; Mallory, M.; Hashimoto, M.; Takeda, A.; Sagara, Y.; Sisk, A.; Mucke, L. Dopaminergic loss and inclusion body formation in α-synuclein mice: implications for neurodegenerative disorders. *Science* **2000**, *287*, 1265–1269.
(23) Uversky, V. N.; Li, J.; Fink, A. L. Metal-triggered structural transformations, aggregation, and fibrillation of human α-synuclein a possible molecular link between parkinson s disease and heavy metal exposure. *Journal of Biological Chemistry* **2001**, *276*, 44284–44296.
(24) Hegde, M. L.; Vasudevaraju, P.; Rao, K. J. DNA induced folding/fibrillation of alpha-synuclein: new insights in Parkinson's disease. *Frontiers in bioscience (Landmark edition)* **2010**, *15*, 418–436.
(25) Grassi, D.; Howard, S.; Zhou, M.; Diaz-Perez, N.; Urban, N. T.; Guerrero-Given, D.; Kamasawa, N.; Volpicelli-Daley, L. A.; LoGrasso, P.; Lasmézas, C. I. Identification of a highly neurotoxic α-synuclein species inducing mitochondrial damage and mitophagy in Parkinson's disease. *Proceedings of the National Academy of Sciences* **2018**, *115*, E2634–E2643.
(26) Giasson, B. I.; Murray, I. V.; Trojanowski, J. Q.; Lee, V. M.-Y. A hydrophobic stretch of 12 amino acid residues in the middle of α-synuclein is essential for filament assembly. *Journal of Biological Chemistry* **2001**, *276*, 2380–2386.
(27) Fusco, G.; Chen, S. W.; Williamson, P. T.; Cascella, R.; Perni, M.; Jarvis, J. A.; Cecchi, C.; Vendruscolo, M.; Chiti, F.; Cremades, N., et al. Structural basis of membrane disruption and cellular toxicity by α-synuclein oligomers. *Science* **2017**, *358*, 1440–1443.
(28) Gonçalves, S.; Outeiro, T. F. Assessing the subcellular dynamics of alpha-synuclein using photoactivation microscopy. *Molecular neurobiology* **2013**, *47*, 1081–1092.

(29) Hegde, M. L.; Rao, K. J. Challenges and complexities of α-synuclein toxicity: new postulates in unfolding the mystery associated with Parkinson's disease. *Archives of biochemistry and biophysics* **2003**, *418*, 169–178.
(30) Nandi, P.; Leclerc, E; Nicole, J.-C.; Takahashi, M DNA-induced partial unfolding of prion protein leads to its polymerisation to amyloid. *Journal of molecular biology* **2002**, *322*, 153–161.
(31) Siddiqui, A.; Chinta, S. J.; Mallajosyula, J. K.; Rajagopolan, S.; Hanson, I.; Rane, A.; Melov, S.; Andersen, J. K. Selective binding of nuclear alpha-synuclein to the PGC1alpha promoter under conditions of oxidative stress may contribute to losses in mitochondrial function: implications for Parkinson's disease. *Free Radical Biology and Medicine* **2012**, *53*, 993–1003.
(32) Hagel, L. Gel-filtration chromatography. *Current protocols in molecular biology* **1998**, *44*, 10–9.
(33) Ó'Fágáin, C.; Cummins, P. M.; O'Connor, B. F. Gel-filtration chromatography. *Protein chromatography: Methods and protocols* **2011**, 25–33.
(34) Nationalencyklopedin. Ljusabsorptionsspektrometri., [Online; accessed 04-April-2018], 2018.
(35) Nationalencyklopedin. Bouguer–Lambert–Beers lag., [Online; accessed 04-April-2018], 2018.
(36) McNaught, A. D.; Wilkinson., A., *Compendium of Chemical Terminology*; Blackwell Scientific Publications, Oxford: 1997.
(37) Demchenko, A. P., *Ultraviolet spectroscopy of proteins*; Springer Science & Business Media: 2013.
(38) Shipman, J.; Wilson, J.; Higgins, C., *An introduction to physical science*; Nelson Education: 2012.
(39) Sutherland, J. C. Linear dichroism of DNA: Characterization of the orientation distribution function caused by hydrodynamic shear. *Analytical biochemistry* **2017**, *523*, 24–31.
(40) Nordén, B., *Circular dichroism and linear dichroism*; Oxford University Press, USA: 1997; Vol. 1.
(41) Rodgers, D. S., *Circular Dichroism: Theory and Spectroscopy*; Nova Science Publishers: 2014.
(42) Goldfarb, A. R.; Saidel, L. J.; Mosovich, E., et al. The ultraviolet absorption spectra of proteins. *Journal of Biological Chemistry* **1951**, *193*, 397–404.
(43) Greenfield, N. J. Using circular dichroism spectra to estimate protein secondary structure. *Nature protocols* **2006**, *1*, 2876.
(44) Rodger, A. How to study DNA and proteins by linear dichroism spectroscopy. *Science progress* **2008**, *91*, Copyright - Copyright Science Reviews 2000 Ltd Dec 2008; Last updated - 2012-12-27, 377.
(45) Cheng, X.; Joseph, M. B.; Covington, J. A.; Dafforn, T. R.; Hicks, M. R.; Rodger, A. Continuous-channel flow linear dichroism. *Analytical Methods* **2012**, *4*, 3169–3173.
(46) Chemistry, U., *An Introduction to Fluorescence Spectroscopy*; PerkinElmer, Inc. UK.: 2000; Vol. 1.
(47) Valeur, B.; Berberan-Santos, M. N., *Molecular fluorescence: principles and applications*; John Wiley & Sons: 2012.

(48) Lindgren, M.; Sörgjerd, K.; Hammarström, P. Detection and characterization of aggregates, prefibrillar amyloidogenic oligomers, and protofibrils using fluorescence spectroscopy. *Biophysical journal* **2005**, *88*, 4200–4212.
(49) Khurana, R.; Coleman, C.; Ionescu-Zanetti, C.; Carter, S. A.; Krishna, V.; Grover, R. K.; Roy, R.; Singh, S. Mechanism of thioflavin T binding to amyloid fibrils. *Journal of structural biology* **2005**, *151*, 229–238.
(50) Biancalana, M.; Koide, S. Molecular mechanism of Thioflavin-T binding to amyloid fibrils. *Biochimica et Biophysica Acta (BBA)-Proteins and Proteomics* **2010**, *1804*, 1405–1412.
(51) Westerlund, F.; Persson, F.; Fritzsche, J.; Beech, J. P.; Tegenfeldt, J. O. In *Single Molecule Analysis*; Springer: 2018, pp 173–198.
(52) Frykholm, K.; Nyberg, L. K.; Westerlund, F. Exploring DNA–protein interactions on the single DNA molecule level using nanofluidic tools. *Integrative Biology* **2017**, *9*, 650–661.
(53) Persson, F.; Fritzsche, J.; Mir, K. U.; Modesti, M.; Westerlund, F.; Tegenfeldt, J. O. Lipid-based passivation in nanofluidics. *Nano letters* **2012**, *12*, 2260–2265.
(54) Ji, S., *Molecular theory of the living cell: Concepts, molecular mechanisms, and biomedical applications*; Springer Science & Business Media: 2012.
(55) Silva, L. P. Imaging proteins with atomic force microscopy: an overview. *Current protein & peptide science* **2005**, *6*, 387–395.
(56) Lekka, M., *Cellular Analysis by Atomic Force Microscopy*; CRC Press: 2017.
(57) Pang, D.; Thierry, A. R.; Dritschilo, A. DNA studies using atomic force microscopy: capabilities for measurement of short DNA fragments. *Frontiers in molecular biosciences* **2015**, *2*, 1.
(58) Bezanilla, M.; Manne, S.; Laney, D. E.; Lyubchenko, Y. L.; Hansma, H. G. Adsorption of DNA to mica, silylated mica, and minerals: characterization by atomic force microscopy. *Langmuir* **1995**, *11*, 655–659.
(59) Werner, T.; Kumar, R.; Horvath, I.; Scheers, N.; Wittung-Stafshede, P. Abundant fish protein inhibits α-synuclein amyloid formation. *Scientific reports* **2018**, *8*, 5465.
(60) Yoe, J. H. The analytical uses of ethylenediaminetetraacetic acid. *Journal of the American Chemical Society* **1958**, *80*, 2600–2600.

A

Appendix 1

Here, complementary data from CD sample preparations and results from CD experiments are presented.

A.1 Circular dichroism sample preparation

Table A.1: Concentrations and volumes of DNA, αS and TE-buffer in CD samples, where the DNA was added into the sample during the experiment. Stock concentration of ctDNA used was 79.0 μM bp and the stock concentration of αS was 51.0 μM.

Sample	**αS conc. [μM]**	**ctDNA conc. [μM bp]**	**αS vol. [μl]**	**TE-buffer vol. [μl]**	**ctDNA vol. [μl]**
αS 1:0	10.0	0.0	58.8	241.0	0.0
αS ctDNA 1:0.25	10.0	2.50	58.8	241.0	10.0
αS ctDNA 1:0.5	10.0	5.0	58.8	241.0	20.0
αS ctDNA 1:0.75	9.0	7.5	58.8	241.0	30.0
αS ctDNA 1:0.9	9.0	9.0	58.8	241.0	40.0
αS ctDNA 1:1.1	8.0	11.0	58.8	241.0	50.0

Table A.2: Concentrations and volumes of DNA, αS and TE-buffer in CD samples, where the DNA was added into the sample during the experiment. Stock concentration of ctDNA used was 214.0 μM bp and the stock concentration of αS was 61.2 μM.

Sample	**αS conc. [μM]**	**ctDNA conc. [μM bp]**	**αS vol. [μl]**	**TE-buffer vol. [μl]**	**ctDNA vol. [μl]**
αS 1:0	12.2	0.0	50.0	200.0	0.0
αS ctDNA 1:0.5	12.0	4.3	50.0	200.0	5.0
αS ctDNA 1:2	11.1	19.9	50.0	200.0	25.0
αS ctDNA 1:5	9.7	45.2	50.0	200.0	65.0
αS ctDNA 1:8	8.4	69.0	50.0	200.0	115.0
αS ctDNA 1:12	7.2	90.1	50.0	200.0	175.0

A.2 Circular dichroism further results

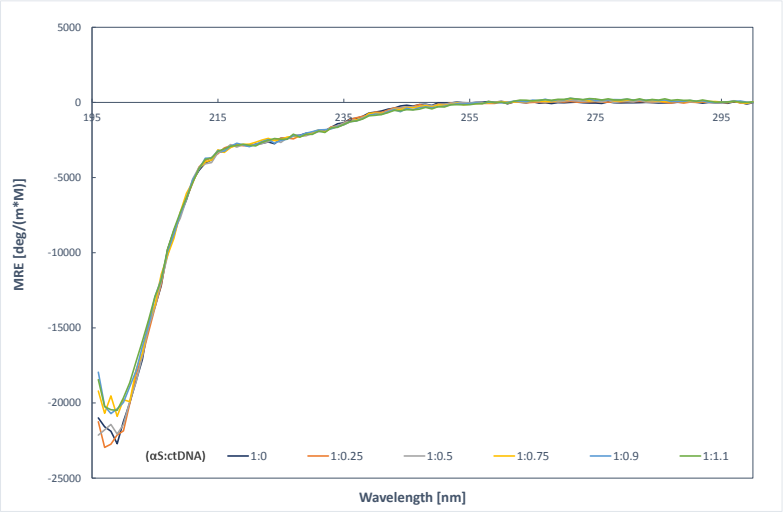

Figure A.1: CD spectra of αS ($\sim$10 μM) together with various concentrations of ctDNA. The changes in signal detected are most likely due to noise created by low wavelengths and high concentration of protein.

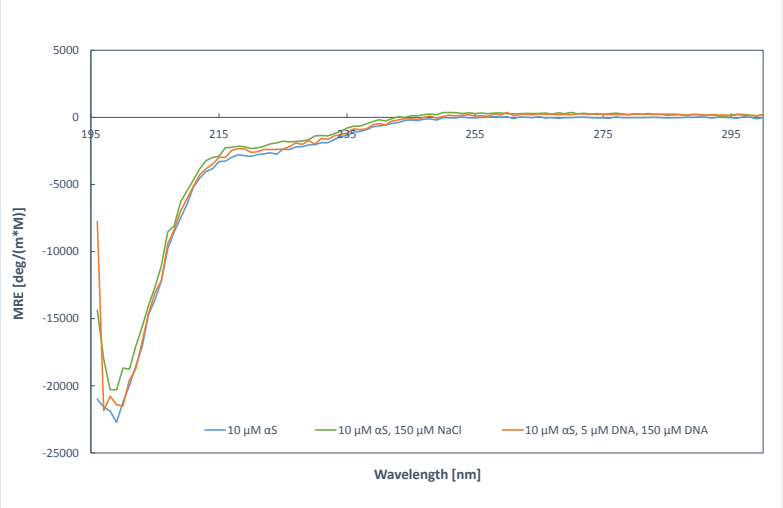

Figure A.2: CD spectra visualising 3 samples; 10 μM αS, 10 μM αS with 150 μM NaCl and 10 μM αS with 150 μM NaCl and 5 μM bp ctDNA. The spectra show no differences in signal when NaCl and DNA are added.

B

Appendix 2

Here, complementary data from LD sample preparations and results from LD experiments are presented.

B.1 Linear dichroism sample preparation

Table B.1: Concentrations of DNA, αS, YOYO and NaCl in LD samples, where the ctDNA concentration was set to 10 μM.

Sample	**αS conc. [μM]**	**DNA conc. [μM bp]**	**YOYO conc. [μM]**	**NaCl conc. [μM]**
ctDNA 1:0	0.0	10.0	0.0	0.0
ctDNA αS 1:0.04	0.4	10.0	0.0	0.0
ctDNA αS 1:1	10.0	10.0	0.0	0.0
ctDNA αS 1:2	20.0	10.0	0.0	0.0
ctDNA αS 1:4	40.0	10.0	0.0	0.0
ctDNA αS YOYO 1:0	0.0	10.0	0.2	0.0
ctDNA αS YOYO 1:0.04	0.4	10.0	0.2	0.0
ctDNA αS YOYO 1:2	20.0	10.0	0.2	0.0
ctDNA αS NaCl 1:2	20.0	10.0	0.0	150.0

Table B.2: Volumes of ctDNA, αS, YOYO and NaCl in LD samples, where the ctDNA concentration was set to 10 μM. The stock concentration of ctDNA used was 214.0 μM bp and the stock concentration of αS was 151.84 μM.

Sample	**αS vol. [μl]**	**ctDNA vol. [μl]**	**YOYO vol. [μl]**	**NaCl vol. [μl]**	**TE-buffer vol. [μl]**
ctDNA 1:0	0.0	63.9	0.0	0.0	1231.1
ctDNA αS 1:0.04	3.7	63.9	0.0	0.0	1227.4
ctDNA αS 1:1	92.2	63.9	0.0	0.0	1138.4
ctDNA αS 1:2	184.4	63.9	0.0	0.0	1046.7
ctDNA αS 1:4	368.8	63.9	0.0	0.0	862.3
ctDNA αS YOYO 1:0	0.0	63.9	56.0	0.0	1280.1
ctDNA αS YOYO 1:0.04	3.7	63.9	56.0	0.0	1276.4
ctDNA αS YOYO 1:2	184.4	63.9	56.0	0.0	1095.7
ctDNA αS NaCl 1:2	184.4	63.9	0.0	105.0	1151.7

B.2 Linear dichroism further results

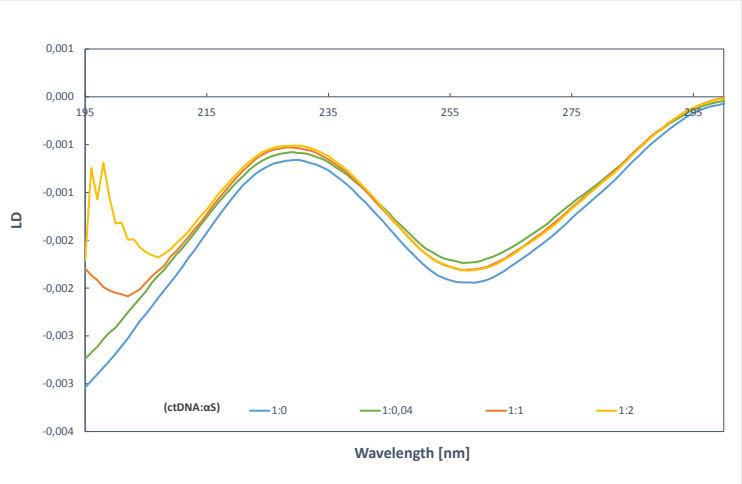

Figure B.1: LD spectra showing the results from all samples after 1 hour our of incubation with ctDNA (10 μM bp) and αS in various concentrations. The increase of signal in the 200-190 nm region for the samples with DNA and αS indicates the presence protein-DNA interactions.

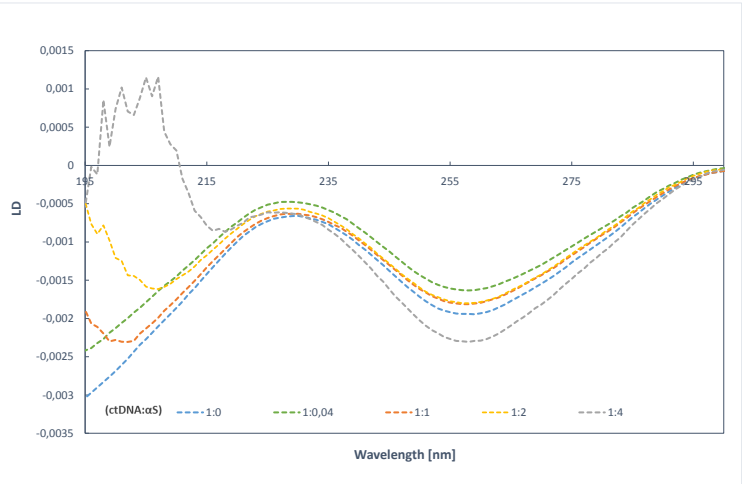

Figure B.2: LD spectra showing the results from all samples after 24 hours our of incubation with ctDNA (10 μM bp) and αS in various concentrations. The increase of signal in the 200-190 nm region for the samples with DNA and αS indicates the presence protein-DNA interactions.

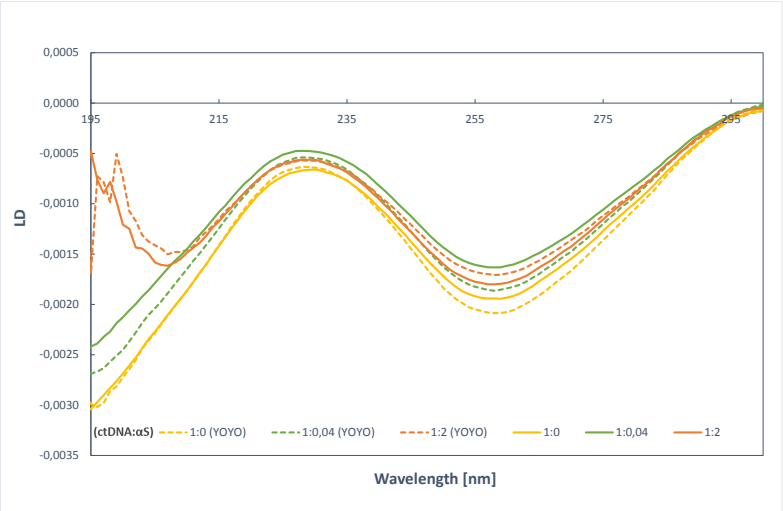

Figure B.3: LD spectra visualising 3 samples of ctDNA (10 μM bp) and αS with and without YOYO (0.2 μM). The spectra show no apparent difference in signal when YOYO is added.

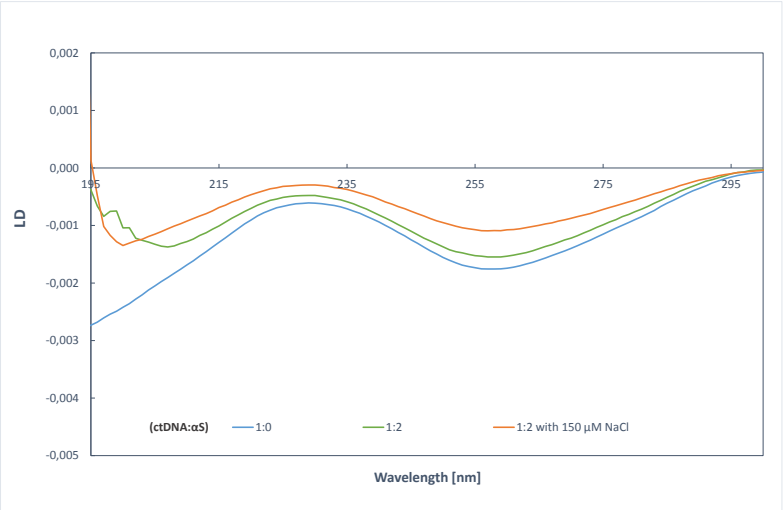

Figure B.4: LD spectra visualising 3 samples of ctDNA (10 μM bp) and αS, where one is with 150 μM NaCl. The spectra show no apparent difference in signal when NaCl is added.

C

Appendix 3

Here, complementary data from AFM sample preparations and results from AFM experiments are presented.

C.1 Atomic force microscopy sample preparation

Table C.1: Concentrations of DNA and αS in AFM samples, where the DNA concentration was set to 5 μM bp.

Sample	**αS conc. [μM]**	**DNA conc. [μM bp]**
1k DNA 1:0	0.0	5.0
1k DNA 1:0.02	0.1	5.0
1k DNA 1:0.2	1.0	5.0
1k DNA 1:2	10.0	5.0
10k DNA 1:0	0.0	5.0
10k DNA 1:0.02	0.1	5.0
10k DNA 1:0.2	1.0	5.0
10k DNA 1:2	10.0	5.0

Table C.2: Volumes of 1k DNA, 10k DNA and αS in AFM samples, where the DNA concentration was set to 5 μM bp. The stock concentration of DNA used was 760.9 μM bp and the stock concentration of αS was 51.0 μM

Sample	**αS vol. [μl]**	**ctDNA vol. [μl]**	**TE-buffer vol. [μl]**
1k DNA 1:0	0.00	0.46	69.55
1k DNA 1:0.02	0.11	0.46	69.43
1k DNA 1:0.2	1.14	0.46	68.40
1k DNA 1:2	11.44	0.46	58.11
10k DNA 1:0	0.00	0.46	69.55
10k DNA 1:0.02	0.11	0.46	69.43
10k DNA 1:0.2	1.14	0.46	68.40
10k DNA 1:2	11.44	0.46	58.11

C.2 Atomic force microscopy further results

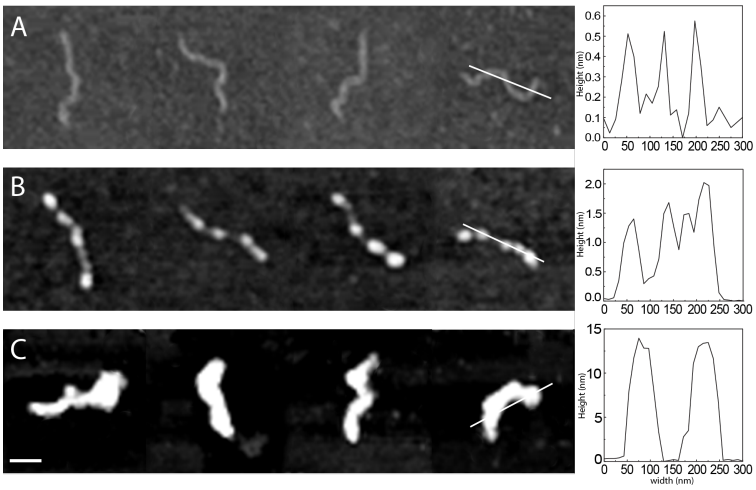

Figure C.1: AFM images of samples of αS (A 0 μM, B 0.1 μM and C 40μM) and 1k DNA (5 μM bp). Image A shows DNA on a Mica surface where the DNA height is estimated to $\sim$0.5 nm. Image B shows DNA on a silica surface where the DNA+αS height is estimated to $\sim$1.5 nm. Image C shows DNA on a silica surface where the DNA+αS height is estimated to $\sim$15 nm.

D

Appendix 4

Here, complementary data from aggregation study preparations and results from aggregation study are presented.

D.1 Aggregation sample preparation

Table D.1: Concentrations of αS, ctDNA, NaCl, ThT and TE-buffer in samples used in ThT assay aggregation experiments.

Sample	**αS conc. [μM]**	**ctDNA conc. [μM bp]**	**NaCl conc. [μM]**	**ThT conc. [μM]**	**Colour code**
αS	50.0	0.0	150.0	13.5	Orange
αS DNA 1:0.02	50.0	0.5	150.0	13.5	Green
αS DNA 1:0.5	50.0	12.5	150.0	13.5	Green
αS DNA 1:1	50.0	25.0	150.0	13.5	Green
αS DNA 1:2	50.0	50.0	150.0	13.5	Green
DNA 0.02	0.0	0.5	150.0	13.5	Blue
DNA 1:0.5	0.0	12.5	150.0	13.5	Blue
DNA 1:1	0.0	25.0	150.0	13.5	Blue
DNA 1:2	0.0	50.0	150.0	13.5	Blue
ThT-NaCl	0.0	0.0	0.0	13.5	Blue
ThT	0.0	0.0	150.0	13.5	Blue

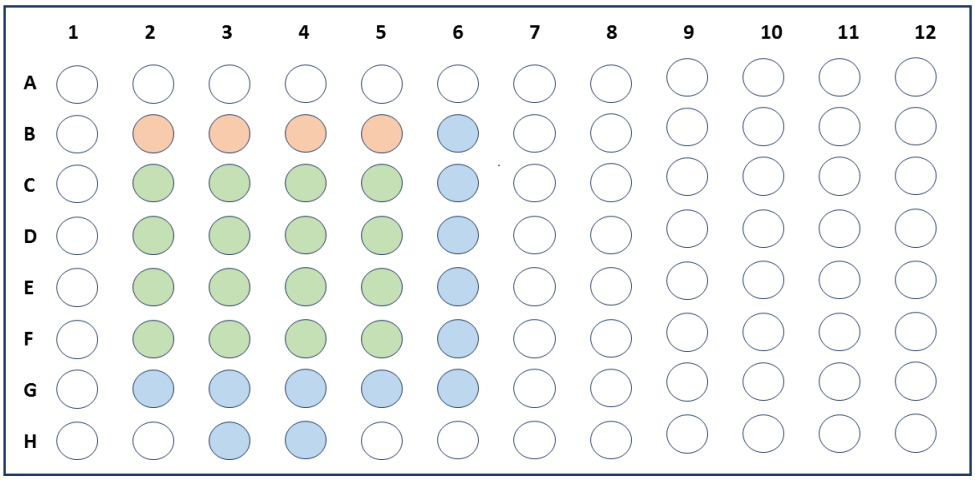

Figure D.1: Location of samples in wells in aggregation experiments, the wells on the edges were not used due to the risk of evaporation. Orange represents αS controls, green represents the samples and blue represents the DNA and ThT controls.

D.2 Aggregation study further results

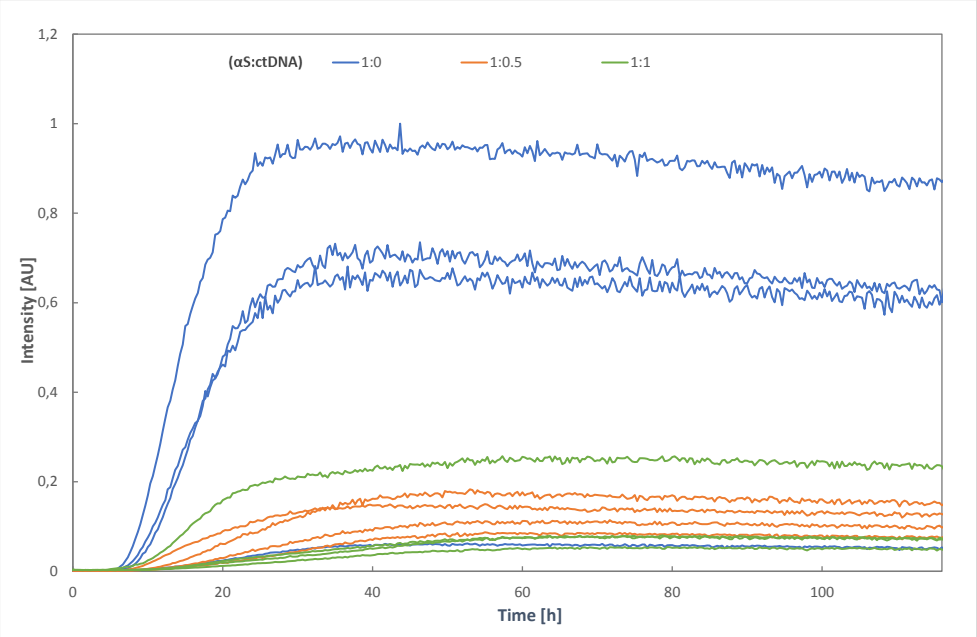

Figure D.2: Aggregation study using ThT assay with samples of αS (50 μM) together with ctDNA (25 μM bp and 50 μM bp) and NaCl (150 μM).

E

Appendix 5

Here, complementary data from NC sample preparations and results from NC experiments are presented.

E.1 Nanofluidic channel sample preparation

Table E.1: Concentrations of αS, DNA and YOYO in samples used in NC experiments.

Sample	**αS conc. [μM]**	**DNA conc. [μM bp]**	**YOYO conc. [μM]**
λ-DNA 1:0	0.0	5.0	0.2
λ-DNA 1:0.2	1.0	5.0	0.2
λ-DNA 1:1	5.0	5.0	0.2
λ-DNA 1:3	15.0	5.0	0.2
λ-DNA 1:8	40.0	5.0	0.2

Table E.2: Volumes of λ-DNA, αS, YOYO and TE-buffer used in NC samples, where the DNA concentration was set to 5 μM bp. The stock concentration of λ-DNA used was 431.0 μM bp and the stock concentration of αS was 51.0 μM

Sample	**αS vol. [μl]**	**λS-DNA vol. [μl]**	**YOYO vol. [μl]**	**TE-buffer vol. [μl]**
λ-DNA 1:0	0.0	0.58	2.0	47.42
λ-DNA 1:0.2	0.99	0.58	2.0	46.43
λ-DNA 1:1	4.9	0.58	2.0	42.52
λ-DNA 1:3	14.7	0.58	2.0	32.72
λ-DNA 1:8	39.2	0.58	2.0	8.22